AD NUMBER

ADB019117

LIMITATION CHANGES

TO:

Approved for public release; distribution is unlimited.

FROM:

Distribution authorized to U.S. Gov't. agencies only; Test and Evaluation; AUG 1976. Other requests shall be referred to Air Force Avionics Lab., Wright-Patterson AFB, OH 45433.

AUTHORITY

WL/AFSC ltr, 21 Feb 1991

AFAL-TR-76-191

HIGH DATA-RATE MULTIPLEXER DEVELOPMENT

NORTHROP RESEARCH AND TECHNOLOGY CENTER
HAWTHORNE, CALIFORNIA 90250

MARCH 1977

TECHNICAL REPORT AFAL-TR-76-191
FINAL REPORT FOR PERIOD NOVEMBER 1974 - JUNE 1976

AIR FORCE AVIONICS LABORATORY
AIR FORCE WRIGHT AERONAUTICAL LABORATORIES
AIR FORCE SYSTEMS COMMAND
WRIGHT-PATTERSON AIR FORCE BASE, OHIO 45433

NOTICE

When Government drawings, specifications, or other data are used for any purpose other than in connection with a definitely related Government procurement operation, the United States Government thereby incurs no responsibility nor any obligation whatsoever; and the fact that the government may have formulated, furnished, or in any way supplied the said drawings, specifications, or other data, is not to be regarded by implication or otherwise as in any manner licensing the holder or any other person or corporation, or conveying any rights or permission to manufacture, use, or sell any patented invention that may in any way be related thereto.

Publication of this report does not constitute Air Force approval of the report's findings or conclusions. It is published only for the exchange and stimulation of ideas.

David G. McLaine

DAVID G. McLAINE
Project Engineer

Donald S Rees

DONALD S. REES, Acting Chief
Microwave Technology Branch
Electronic Technology Division
Air Force Avionics Laboratory

Copies of this report should not be returned unless return is required by security considerations, contractual obligations, or notice on a specific document.

UNCLASSIFIED

SECURITY CLASSIFICATION OF THIS PAGE (When Data Entered)

REPORT DOCUMENTATION PAGE

READ INSTRUCTIONS BEFORE COMPLETING FORM

1. REPORT NUMBER: AFAL-TR-76-191
2. GOVT ACCESSION NO.
3. RECIPIENT'S CATALOG NUMBER: Rept.
4. TITLE (and Subtitle): High Data-Rate Multiplexer Development
5. TYPE OF REPORT & PERIOD COVERED: Final Nov 74 - Jun 76
6. PERFORMING ORG. REPORT NUMBER
7. AUTHOR(s): A. Bahraman
8. CONTRACT OR GRANT NUMBER(s): F33615-75-C-1032
9. PERFORMING ORGANIZATION NAME AND ADDRESS: Northrop Research and Technology Center, Hawthorne, CA 90250
10. PROGRAM ELEMENT, PROJECT, TASK AREA & WORK UNIT NUMBERS: 17030
11. CONTROLLING OFFICE NAME AND ADDRESS: AFAL/DHE, AFAL/Wright-Patterson AFB, Ohio
12. REPORT DATE: March 1977
13. NUMBER OF PAGES: 95
14. MONITORING AGENCY NAME & ADDRESS (if different from Controlling Office): 200p.
15. SECURITY CLASS. (of this report): Unclassified
15a. DECLASSIFICATION/DOWNGRADING SCHEDULE

16. DISTRIBUTION STATEMENT (of this Report)

Distribution limited to US Government agencies only; test and evaluation; August 1976. Other requests for this document must be referred to AFAL/DHM, Wright-Patterson AFB, OH 45433.

17. DISTRIBUTION STATEMENT (of the abstract entered in Block 20, if different from Report)

18. SUPPLEMENTARY NOTES

19. KEY WORDS (Continue on reverse side if necessary and identify by block number)

Electron Beam Semiconductor
EBS
Multiplexer
High Data Rate
Modulator Driver

20. ABSTRACT (Continue on reverse side if necessary and identify by block number)

The significance of this research and development to the Air Force is that an Electron-Beam-Semiconductor (EBS) digital multiplexer has been developed which has the capability of achieving output data rates exceeding 2 Gbits/sec. Two design approaches are presented for multiplexing multiple input data lines into a single output (parallel-to-serial conversion) with 2 Gbits/sec serial output data rate. The first approach uses a CRT-type electron gun, eight input gates, and one silicon diode target. The second approach uses multiple electron sources, multiple input gates, and a single silicon diode target. A gating

DD FORM 1 JAN 73 1473 EDITION OF 1 NOV 68 IS OBSOLETE

UNCLASSIFIED

SECURITY CLASSIFICATION OF THIS PAGE (When Data Entered)

407696

system is used to present to the target a 0.5-ns aperture time per electron gun. This approach is much less sensitive to misalignment and power supply and RF input drive instabilities than the first approach. In addition, higher output signal amplitudes and a smaller tube are achieved. Output pulse characteristics demonstrated at 2 Gbits/sec data rate are 5 to 7V pulse amplitude into a 50 ohm load and less than 0.25-ns pulse risetime.

FOREWORD

The author would like to express his appreciation to others who have contributed to this program. Many thanks to Mr. Steven Chang for his valuable contributions in target fabrication. The author would also like to thank Mr. David G. McLaine of the Avionics Laboratory and Dr. Klaus K. Schuegraf for their continuous support during the course of this program. Mr. R. L. Tanquary built most of the experimental hardware and the two multiplexer tubes. Target fabrication and processing was performed by Mrs. E. Szoke and Mr. N. Goodwin.

This Final Report, submitted pursuant to the performance requirements of Contract No. F33615-75-C-1032, contains a description including details of construction, function and operation of an invention for an E-Beam Multiplexer which Northrop asserts was first conceived and first actually reduced to practice at Contractor's private expense prior to award of aforementioned contract, which invention is described, shown and claimed in U. S. Patent Application Serial Number 251018 filed 8 May 1972 under the title "High Speed Deflection Modulated Electron Beam Signal Processor" by Walter E. Crandall et al.

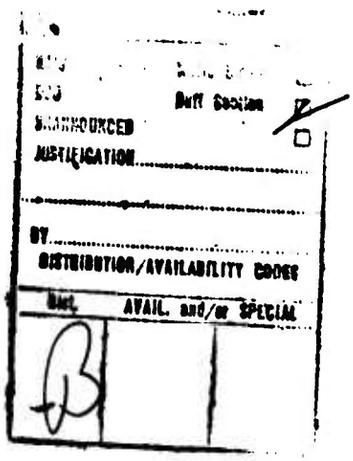

TABLE OF CONTENTS

LIST OF ILLUSTRATIONS

ILLUSTRATIONS (Continued)

ILLUSTRATIONS (Continued)

SECTION I
INTRODUCTION

Future aerospace communications systems will be required to relay digital data at multi-gigabit/sec rates. These systems would be used to transmit large amount of information from one terminal to another within a short time frame. For best system efficiency it becomes desirable to develop a high data rate technology to a point where a one-carrier frequency system will be able to handle multi-gigabit/sec data rates. Recently, PIN diodes with switching speeds approaching 2 Gbits/sec have been developed as modulators for a millimeter-wave carrier in biphase or quadraphase phase-shift-keying systems.[1] However, a sufficiently fast PIN driver is needed in order to make a multi-Gbit/sec digital communication system realizable. Conventional solid-state devices cannot satisfy this requirement due to limitations in their power-frequency capabilities. This report describes the development of two Electron Beam Semiconductor (EBS) digital multiplexers capable of driving a PIN diode modulator at data rates of 2 Gbits/sec or higher.

The primary objective of this program is to develop an EBS digital signal processor that can multiplex eight input data lines into a single output line with 2 Gbit/sec serial data rate. The output pulse specifications are 5V signal amplitude and less than 0.2 ns pulse rise-time with 50Ω output impedance. A variable output dc level between 0 and -5V is also desired. The input gates are rated for 50Ω impedance, and 250 Mbits/sec input data are specified. The program effort includes four major tasks.

The primary Task I effort was to consider various approaches to the EBS multiplexer design and define the optimum design on the basis of (a) capability of meeting program specifications, (b) future growth, (c) simplicity and ease of fabrication, and (d) cost. The approaches include single or multiple electron sources, single or multiple targets, and a solid-state multiplexer-EBS-amplifier. Task II effort included the fabrication of one optimum multiplexer.

Task III of the program involved the analysis of various techniques for demultiplexing the data stream generated by the multiplexer of Task II into eight parallel outputs carrying 250 Mbits/sec data. A multiple-gun, single-target EBS multiplexer was designed and built in the Task IV time period.

SECTION II
TECHNICAL APPROACH

A number of alternative system designs have been considered for multiplexing relatively low digital-data rate streams into a single 2 Gbits/sec output stream capable of driving the PIN diode modulator of an RF carrier. In principle, the PIN diode could be incorporated into the multiplexer, but this concept is beyond the scope of this program.

The design approaches to the EBS multiplexer/PIN driver to be discussed stem from our understanding of the basic function of a signal processor, as depicted by the schematic of Figure 1. The multiplexer output pulses are produced by the interaction of an electron beam and a semiconductor target; in turn, the presence of a current pulse at the multiplexer output is determined by the information signals fed at its inputs. In this configuration, addressing information is placed on the electron beam and read at the target. The primary design goal is to multiplex 4-ns-wide input data pulses (250 Mbits/sec) from eight input lines into output pulses of 0.5 ns width and 5V amplitude. The desired output pulse rise-time is 0.2 ns.

The above information processing configuration can be implemented in a number of ways using designs which include one or a combination of the following: (a) single-target, (b) multiple-target, (c) single-electron source (cathode), and (d) multiple-cathode approach. Any approach using a multiple-target design is not expected to meet the output power and rise-time specifications of 5V and 0.2 ns, respectively. We have considered a multiple-gun, single-target approach; a GaAs Transferred Electron Device (TED) multiplexer-EBS amplifier combination; and a single-gun, single-target design. The TED device concept was not developed into hardware and is therefore discussed separately in Section V. The other two approaches are conceptually presented here and in more detail in Sections III and IV.

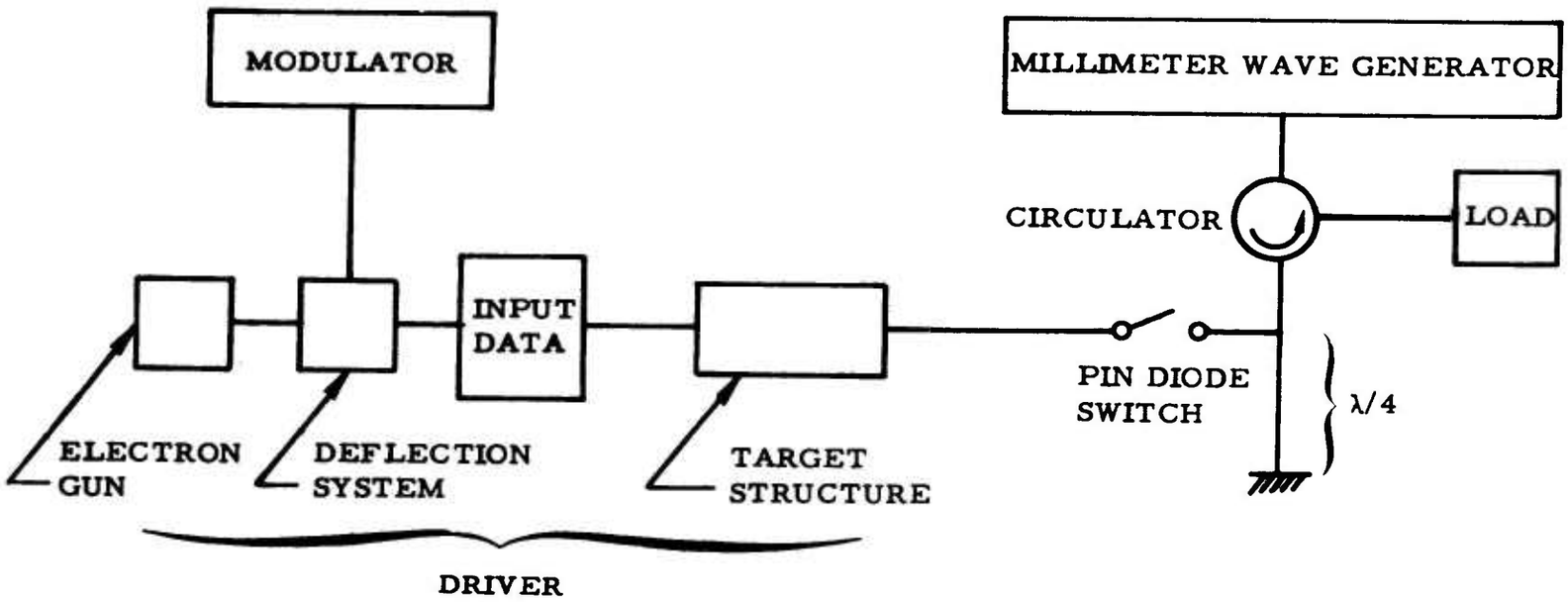

Figure 1. Schematic of the E-Beam Data Processor driving a PIN diode switch.

2.1 SINGLE-GUN, SINGLE-TARGET APPROACH

Figure 2 shows a schematic presentation of our EBS multiplexer design approach. The device includes (1) a CRT-type electron gun which produces a pencil beam, (2) a deflection system which launches the beam into conical rotation about the processor center axis, (3) a gate structure for addressing the beam, (4) an Einzel lens which bends and focuses the beam onto the target, (5) a semiconductor target which is bombarded by the beam and produces the output signal, and (6) a funnel which further focuses and aligns the beam onto the target.

The processor operates in the following manner. The electron gun is biased to provide an electron beam along the axis. A sinusoidal signal (250 MHz) on the deflection system causes the beam to go into conical rotation, i.e., once the beam exits the deflection system, it traces a circle in any plane perpendicular to the center axis. For the input and output rates specified, the gate structure consists of eight pairs of deflection plates mounted in a ring concentric with the center axis, and each pair of plates is a beam address-gate. After emerging from a gate, the electron beam is focused onto the target or deflected away dependent on the polarity of the data pulse on the gate, thus producing a 1 or 0 output data pattern. In this configuration, then, eight input data pulses are read in each beam revolution period of 4 ns. Each input data pulse is 4 ns wide and the corresponding output pulse is 0.5 ns wide. Therefore, eight input lines, each carrying 250 Mbits/sec data, are multiplexed into a single output with 2 Gbits/sec serial data rate.

2.2 MULTIPLE-SOURCE, SINGLE-TARGET APPROACH

In this approach, eight electron sources are focused on a single target, as shown schematically in Figure 3. Each source may be a conventional CRT-type gun or a field emission cathode (FEC) with appropriate electron optics. The latter configuration can result in a small, compact multiplexer if the usual problems of emission instability, noise, short life, and emission non-uniformity associated with FEC arrays can be solved satisfactorily.

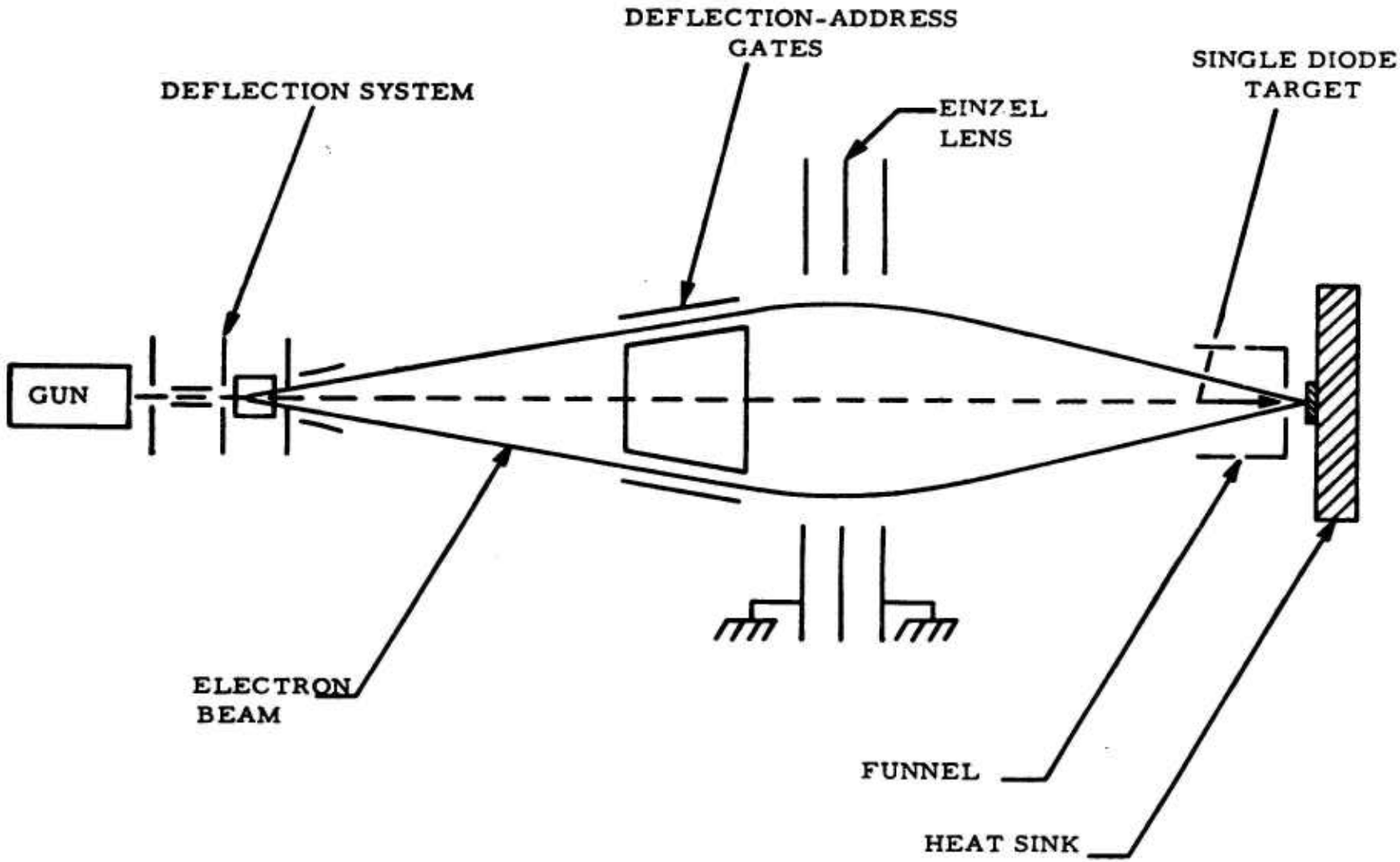

Figure 2. Single-Target Digital Multiplexer

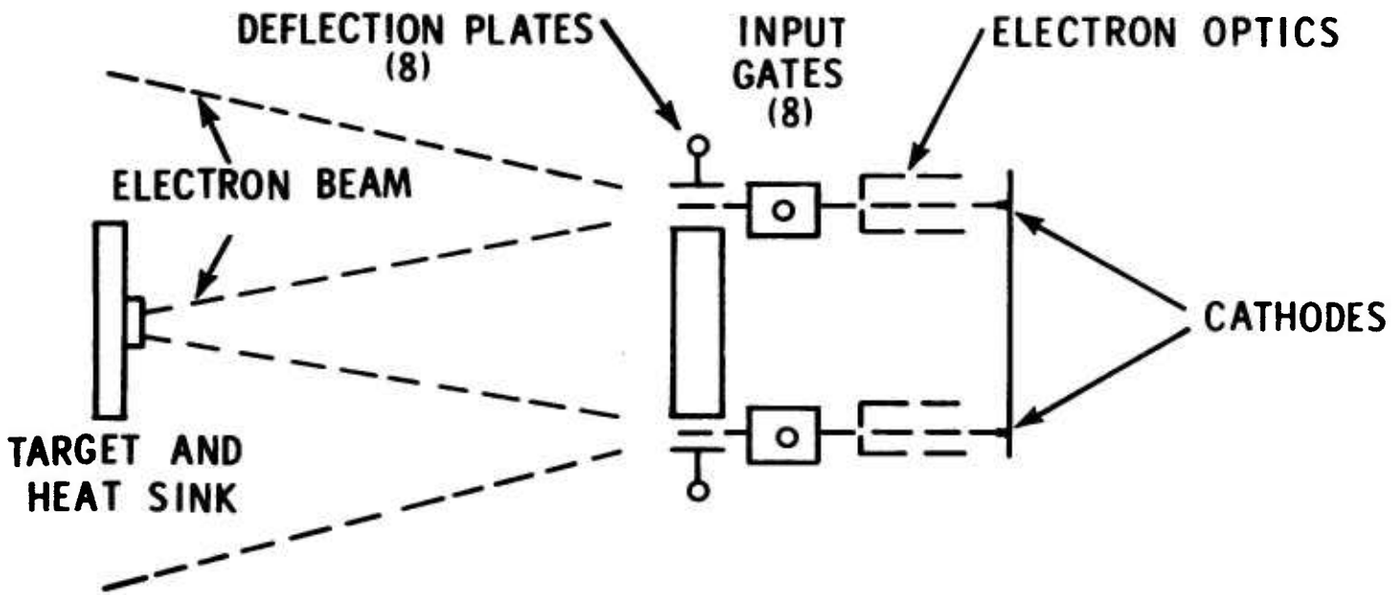

Figure 3. Multiple-Source, Single-Target Design. The electron beam is shown at points of maximum deflection. Only two guns from a circular array of eight are shown. The position of the gates and the deflection plates may be interchanged.

For 2 Gbits/sec output data rate, each output bit pulse width is 0.5 ns and therefore the aperture time per electron source must be 0.5 ns. That is, the eight sources must sequentially generate eight 0.5-ns-wide pulses at the output in 4 ns. Since it is extremely difficult to gate each electron source to turn on for 0.5 ns with an acceptable rise-time, other gating schemes will have to be used, as described below.

A possible scheme is shown in Figure 3. The electron guns are kept on all of the time and two sets of deflection plates are used. One set of eight pairs is used for the input data, and each pair in the other set of eight is resonated at 250 MHz to deflect the beam onto the target for 0.5 ns during the 4-ns, 250-MHz sine-wave period. That is, the target position coincides with the deflection minimum (or maximum). A single amplifier may be used to drive all the eight pairs of deflection plates with 0.5-ns (sine-wave) delay between two adjacent pairs. In this manner, eight equal-amplitude, 0.5-ns-wide pulses are sequentially generated at the target in 4 ns in the absence of any input data pulses. The input data deflection gates are then used to control the output data pattern in accordance with the input data pattern.

A second mode of operation is feasible that reduces the number of guns by a factor of two. The electron beam from each gun is allowed to strike the target at the point of zero RF deflection. Hence, two output pulses are produced per gun in each RF deflection period. For eight bits, then, four electron guns will suffice (see Section IV).

The above schemes with conventional CRT-type guns require about four or eight times as much power as our single-gun, single-target approach and are therefore not as attractive on this basis. However, the multiple-gun design has advantages in device size, ease of fabrication, and alignment of tube components. If the electron source is made in an FEC array, very substantial savings in input power and device size can be realized. In this configuration, an electrode may be used on the FEC chip as an input gate. Thus each FEC is normally off and is turned on by a 4-ns-wide input data pulse.

A pair of deflection plates, resonated at 250 MHz, is again used in front of each FEC to deflect the beam onto the target for only 0.5 ns during the 4-ns input pulse width. This scheme offers low input power and compact device size. However, the input gates need to be isolated at -10 kV, and this may not be possible to achieve broadband at 250 Mbit/sec data rate. To get around the problem, each FEC gate electrode may be resonated at 250 MHz and an additional set of deflection plates introduced as in Figure 3. Very precise synchronization of the input data and the 250 MHz signals in the FEC gate electrode and the deflection plates would be required.

Due to the instability and reliability problems of FEC arrays, a multiple-source FEC design was not considered in this program.

SECTION III
SINGLE-GUN, SINGLE-TARGET MULTIPLEXER

In this section, the design, fabrication and experimental evaluation of the single-gun, single-target EBS multiplexer are described.

3.1 TARGET DESIGN, FABRICATION AND EVALUATION

The target is a single silicon p-n junction diode. The main program requirements in the development of the target are to achieve 5V amplitude and 0.2-ns pulse rise-time into 50Ω when the device is excited by a modulated electron-beam source. Target life under bombardment by 10-keV electrons is also of primary concern. Semiconductor diodes usually show degradation in their reverse current-voltage characteristics in an electron beam environment. The degradation is associated with an increase in reverse current and a decrease in breakdown voltage. This damage is not fundamental and may be prevented by proper design, using a diffused p+ guard-ring and an effective electron beam shield.

Consider a p^+-n-n^+ silicon EBS diode. The output signal amplitude and rise-time determine the target design. The output voltage is (assuming the beam spot is larger than the diode diameter)

$$V = J_B AMR \tag{3-1}$$

where R is the load impedance, M = 2000 is the target multiplication factor, A is the diode active area, and J_B is the beam current density. Assuming $J_B = 50\ mA/cm^2$, R = 50Ω, and V = 5V, Eq. (3-1) yields $A = 10^{-3}\ cm^2$, or a diode radius of 178 μm. The guard-ring will require an additional 12 μm, or a total diode area of $11.4 \times 10^{-4}\ cm^2$. The depletion-layer width W can now be chosen to achieve minimum rise-time.[2] That is,

$$W = \sqrt{2.97\ v_s\ \epsilon AR} \tag{3-2}$$

where v_s is the electron saturation velocity and ϵ is the dielectric permittivity of Si. For $v_s = 7 \times 10^6$ cm/sec (at an electric field of 15 kV/cm), W is 10.9 μm. The minimum rise-time, t_r, is also given by Norris[2]

$$t_r = 1.88\left(\epsilon AR/v_s\right)^{1/2} \tag{3-3}$$

From Eqs. (3-2) and (3-3) we have

$$\begin{aligned} T &= 2.97\,RC \\ t_r &= 3.24\,RC \end{aligned} \tag{3-4}$$

where $T = W/v_s$ is the electron transit-time and C is the diode capacitance. Hence,

$$\begin{aligned} &T = 156\text{ ps},\quad RC = 52.5\text{ ps}, \\ &C = 1.06\text{ pF},\quad t_r = 170\text{ ps} \end{aligned} \tag{3-5}$$

To complete the design, we require that the generated electron concentration just equals the ionized donor concentration in the depletion region. That is[3]

$$n = \frac{M J_B}{e v_s} = N_B = \frac{2 \epsilon E_a}{eW}$$

where n and N_B are the electron and donor concentrations, and E_a is the average junction field when the n-layer is just fully depleted. Then,

$$E_a = \frac{T}{2\epsilon} M J_B .$$

The other parameters are

$$E_a = 7.8\text{ kV/cm}$$

$$V_b = E_s \cdot W + V = 21.5\text{V}$$

$$N_B = 10^{14}/\text{cm}^3$$

$$\rho = 50\ \Omega\text{-cm}$$

Power dissipation in the diode is 1.65W from the power supply, or 14 W/mm^2. The beam power dissipation is 5 W/mm^2; hence the peak diode dissipation is about 20 W/mm^2 and the average value is 10 W/mm^2.

In order to determine the junction depth for the p-diffusion, one may note that the penetration depth of 10-keV electrons in Si is about one micron. The energy loss profile is not linear in the 1 μm region and peaks within this distance.[4] Hence, for efficient carrier multiplication and collection, it is desirable to locate this peak in the depletion region. From the data of Ref. 4, the junction depth (i.e., the thickness of the p^+-layer) should be 0.3 - 0.5 μm.

The above data provide all the necessary information for the fabrication of devices. However, other considerations are needed in order to achieve a reliable device under electron beam bombardment. For unpassivated diodes, direct exposure of the junction depletion region to an e-beam results in an appreciable increase in reverse leakage current. This is probably due to creation of tunneling and/or generation-recombination centers in the junction depletion region at the surface. For SiO_2 passivated diodes, charging of the oxide layer by an electron beam will create a field-induced junction and inversion layer under the oxide and hence will give rise to channel currents and low breakdown voltage. The principal problem is therefore to provide for complete passivation of the device where the p-n junction interfaces the surface. The usual SiO_2 passivation is inadequate as described above. To deal with the problem, we have used two techniques: (1) the use of poly-crystalline silicon for electron charge leakage and as a protective beam shield on the oxide layer, and (2) a p^+-guard-ring at the junction periphery which removes the junction interface at the surface to a more protected region under the oxide. Also, a diffused 0.3-μm p^+ region has a small radius of curvature where the junction reaches the surface. This small radius causes premature breakdown near the surface. The guard-ring provides for a much larger radius of curvature and hence elminates the difficulty. Figure 4. shows a schematic of the target design. The thin metallization in the active region

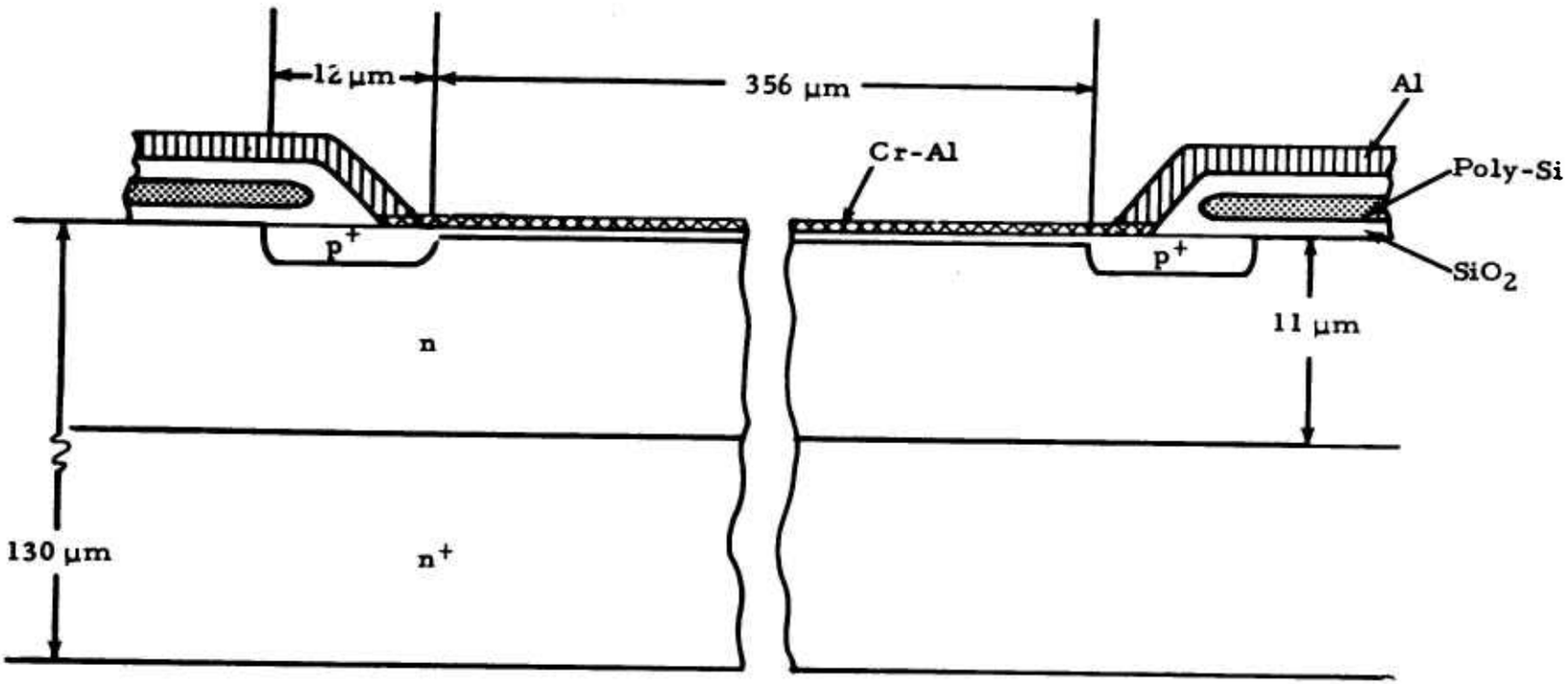

Figure 4. Schematic of the Multiplexer Target

consists of a 20 nm chromium layer and a 50 nm aluminum layer for low contact resistance. The Cr-layer is used to prevent the aluminum -silicon reaction which causes diode failure.

Target fabrication was conducted in-house on Sb-doped n^+-substrates. The processing flow-chart is given in Table 3-I. Problems were encountered in the course of target fabrication which put this phase of the program a few months behind schedule midway through the program.

TABLE 3-I. PROCESS OUTLINE FOR EB-8 TARGET DIODE POLY-SILICON PASSIVATION

- SUBSTRATE PREPARATION
- EPI GROWTH
- OXIDATION (cut guard-ring window)
- P+ DIFFUSION GUARD RING
- THERMAL OXIDE
- POLY SILICON DEPOSITION (cut poly)
- CHECK POLY SLOPE
- OXIDATION (cut P-diffusion window)
- P-DIFFUSION
- MEASURE DIODE I-V CHARACTERISTICS
- ANNEAL 1 HOUR
- MEASURE DIODE I-V CHARACTERISTICS
- METAL DEPOSITION (cut contact pattern)
- ELECTRICAL TEST
- THIN WAFER, DEPOSIT GOLD
- ELECTRICAL TEST

The metallization on most wafers showed a V-shaped crack on the poly-silicon slope when examined by a scanning electron microscope (SEM). After etching the metal layer on a completed wafer, the SEM photograph of Figure 5 was obtained for a typical diode. As is evident in the figure, the poly slope is extremely steep. Photoresist (PR) does not stick well to such steep steps, and during the etching of the metal pattern, the PR does not provide sufficient resistance to the etchant along the step. This problem can be solved by making the poly step with a shallow slope. Considerable effort was spent to achieve a gradual, shallow poly slope, which finally resulted in the successful completion of the target fabrication task according to program goals.

Two different techniques were employed in achieving a gradual poly slope: (1) after etching the poly-silicon layer, phosphorus-doped glass was deposited on the wafer and the glass was subsequently flowed at 1050°C.[5] This provided a smooth coverage of the poly step. However, the results were not uniformly repeatable, and in addition, problems were encountered in etching the shallow p-diffusion window because the phosphorus-doped glass etched too fast compared to the SiO_2 layer on the shallow p-diffusion window. Severe under-etching of the phosphorous-glass layer was observed during this etch step. (2) In the second method, photoresist was used to etch the poly in place of the usual SiO_2 mask, but the resist layer was flowed at ~100°C in order to produce a rounded edge. This technique produced a very gradual poly slope. Figure 6 shows an SEM photograph of a completed target.

The evaluation of the target included measuring the following: diode capacitance-voltage and current-voltage characteristics, multiplication factor under electron-beam bombardment, and rise-time in the EBS mode of operation. The measured capacitances for metallized and unmetallized (on wafer) diodes were substantially different. For example, on wafer lot 6-5-5, the values were 1.25 pF and 1 pF, respectively, at 25V reverse bias. The difference is due to the excess capacitance arising from the diode metal

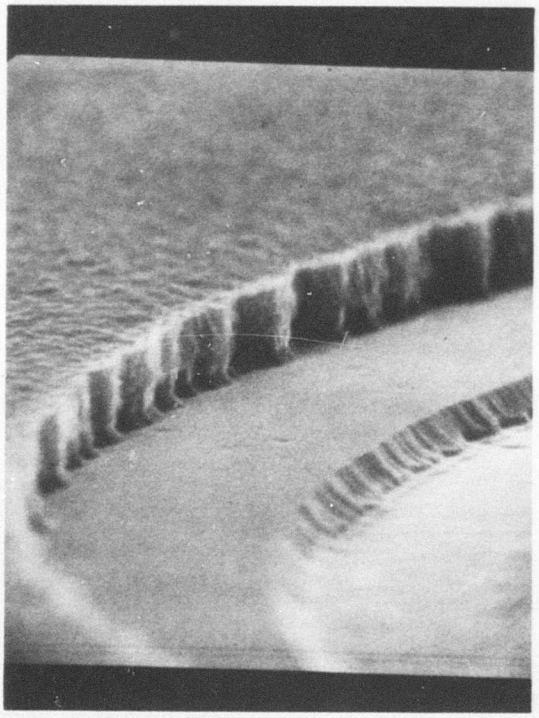

Figure 5. An SEM photograph of the target oxidized poly-silicon step.

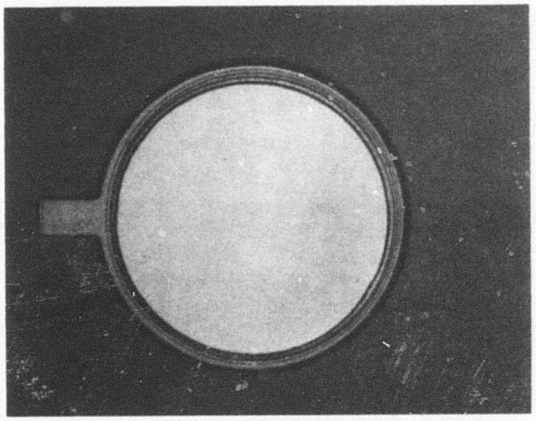

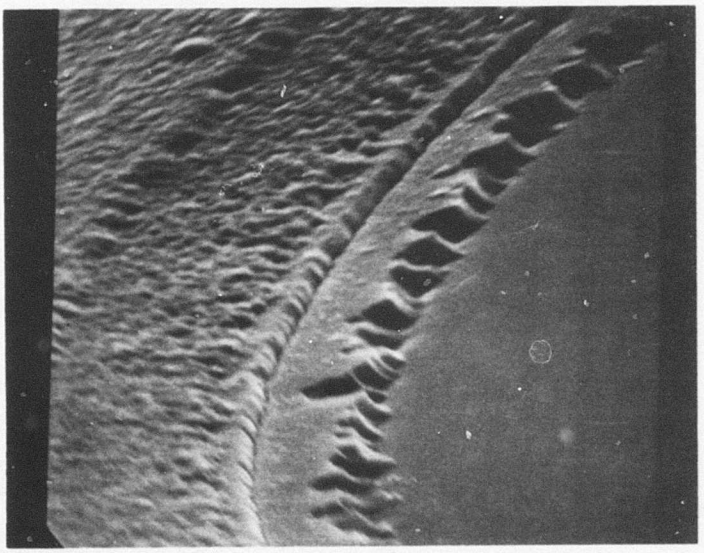

Figure 6. Top: Photograph of a diode of lot 6-5-5.

Bottom: SEM picture of the aluminum metallization.

overlay and contact pad. The epi thickness was increased to 13 μm in order to reduce the diode capacitance and offset the effect of the metal overlay. The breakdown voltage was over 70V and generally averaged about 100V on wafer lot 6-5-6. The measured target gain (electron multiplication factor) was about 1800, slightly below our expectation value of 2000. The difference, however, is well within the experimental error.

The target rise-time was measured by sinusoidally deflecting an electron beam across the target. Figure 7 shows the diode dc and pulse response under electron-beam excitation. The 10 - 90% rise-time is less than 0.2 ns.

3.2 ANALYSIS OF TARGET COOLING

Figure 8 shows a schematic of the target cooling arrangement. When an electron beam of power density 50 mA/cm^2 x 10 kV impinges on the silicon chip, the beam power dissipates within about 1 μm of the chip surface. This heat conducts through the diode and then disperses through the copper base heat sink.

It is desired that the maximum temperature of the chip be below 100°C. The temperature drops from the top of the chip to the ambient air may be estimated as follows.

The peak power dissipation per unit area is 2 kW/cm^2 in a diode area of $11.1 \times 10^{-4} cm^2$. If the chip thickness δ is 150 μm, the diode temperature drop for an average dissipation of $q = 2000\ W/cm^2$ will be (the average value is taken equal to the peak value for design safety)

$$T_1 - T_2 = \frac{q\delta}{k} = \frac{2000 \times 1.5 \times 10^{-2}}{1.15} \approx 26°C.$$

A thermal conductivity of 1.15 W/cm°C for silicon is used.

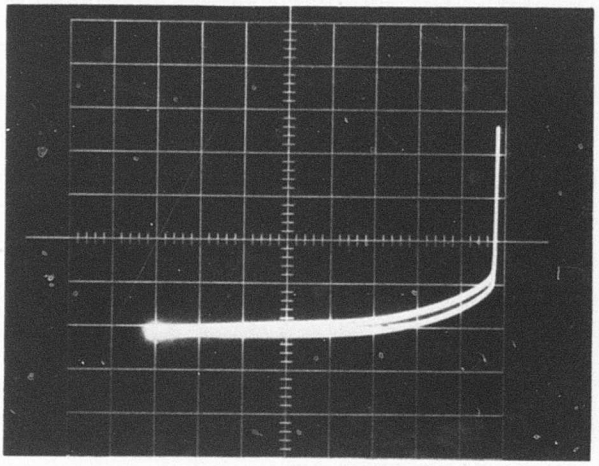

Diode reverse characteristics under electron beam bombardment. Vertical: 20 mA/div., Horizontal: 5V/div.

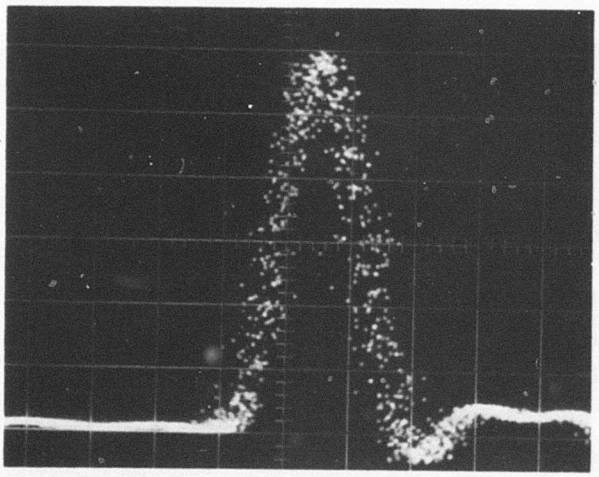

Figure 7. Multiplexer target pulse response measured by S40 sampling head. Vertical: 0.2V/div., Horizontal: 0.2 ns/div. Sampling head rise-time is rated at 40 ps.

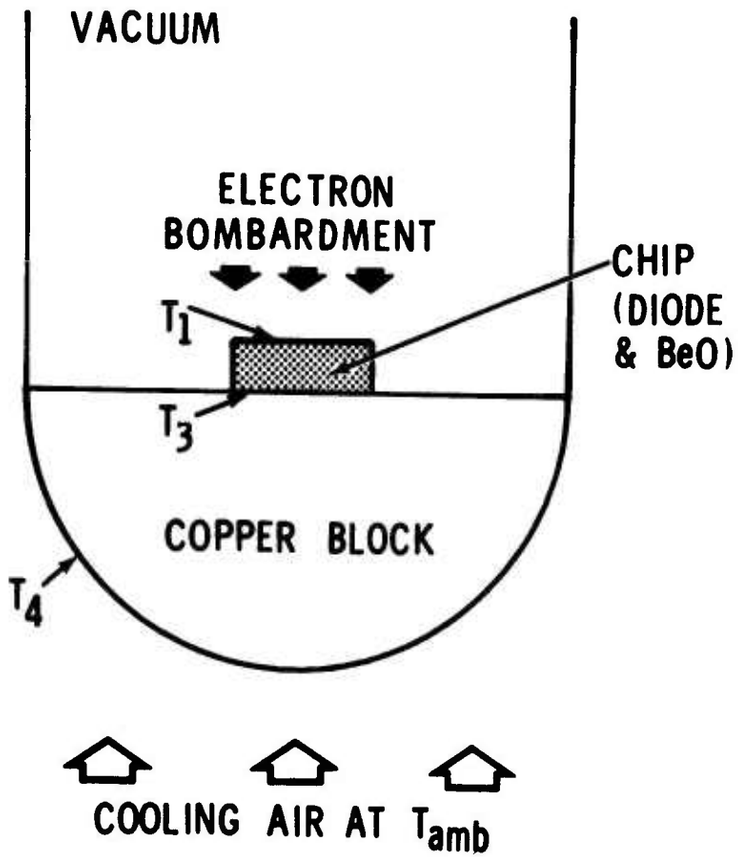

Figure 8. Schematic of a target structure for thermal analysis.

The temperature change across a 10-mil (250 μm) BeO chip is

$$T_2 - T_3 = \frac{q\delta_{beo}}{k_{beo}} = \frac{2000 \times 1.27 \times 10^{-2}}{2.5} \approx 20°C$$

Assuming a hemispherical copper block of 1.5 cm radius under the chip, one can estimate the temperature drop from the chip-copper junction to the outer surface of the hemisphere to be

$$(T_3 - T_4) = \frac{Q_o(b-a)}{2\pi k_{Cu} ab} \approx 5°C$$

where

a = inner radius of the hemisphere, assumed to be 1.8×10^{-2} cm

b = outer radius of the hemisphere, 1.5 cm

Q_o = total heat into the inner hemisphere which is about 2.1 watt

k_{Cu} = copper thermal conductivity, 3.7 W/cm°C.

The temperature drop from the copper surface to the cooling air is

$$T_4 - T_{amb} = \frac{Q_o}{2\pi b^2} \frac{1}{h_{air}} = 15°C$$

where $h_{air} \approx 10^{-2}$ W/cm^2°C is assumed for air at moderate cooling speeds.

Thus the total drop is

$$T_1 - T_{amb} = 26°C + 20°C + 5°C + 15°C = 66°C$$

If 25°C ambient air is assumed, the diode temperature T_1 becomes about 91°C, which is a conservative estimate because no lateral spreading of heat flow was assumed in silicon and in BeO layers and the average power dissipation was assumed equal to the peak value of 2 kW/cm^2.

3.3 TUBE DESIGN AND FABRICATION

The components of the tube include the electron gun, deflection system, deflection-address structure (input gates), unipotential lens, funnel, and target mount. All the components must be coaxially aligned for the proper operation of the multiplexer. In this respect, the alignment of the deflection-address structure is most critical and determines the number of gates that are accessible to the target. The tube components are briefly described below.

Electron Gun. The design requires a gun producing a pencil beam with a current density of 50 mA/cm^2 at the target. Various CRT-type guns were evaluated by measuring their beam profile to determine the beam spot size and variation of current density along the beam cross section. Figure 9 shows a typical beam profile. One CRT-type gun was converted into a Pierce gun using a proper grid design and a BaO-impregnated cathode. Signigicant improvement in the gun output current was achieved. However, the cathode power consumption of ~14W was excessive. Since standard CRT guns satisfying program needs could be obtained commercially, the Pierce gun effort was not pursued further. The CRT-type gun CT94-E, manufactured by Cliftronics, Inc., produced the highest current level and was used in the design.

Deflection System. The satisfactory operation of the signal processor depends very critically on the generation of perfect conical beam rotation. Since magnetic deflection at 250 MHz is difficult to achieve, electrostatic deflection has to be used. The classical double pair of horizontal and vertical deflection plates are inadequate; the centers of deflection of the two pairs of plates are physically apart; hence, one can generate a circle only in one chosen plane perpendicular to the center axis – the rotation pattern is elliptical in any other plane. A system which gave satisfactory results consisted of three pairs of deflection plates, e.g., horizontal-vertical-horizontal deflection plates. Analytical results indicate that by proper design it is possible to have the center for horizontal deflection coincide with that for vertical deflection

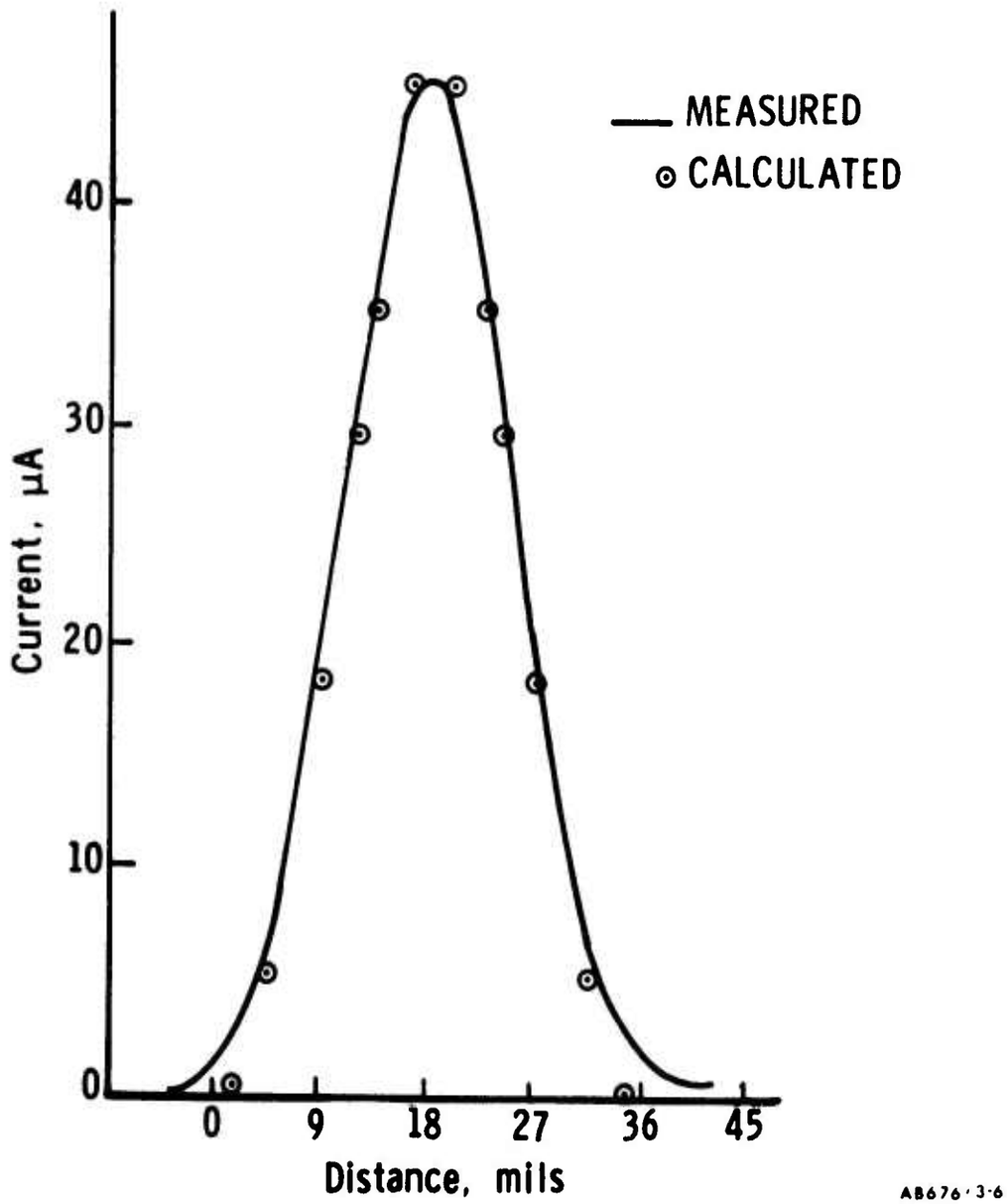

Figure 9. The beam profile of the special CT93E gun with 15-mil grid aperture.

for small deflection angles.[6] The system would therefore achieve the desired conical beam rotation, i.e., a circular beam rotation pattern in any plane perpendicular to the center axis. By properly resonating each pair of deflection plates at 250 MHz, the input power-drive was reduced to less than 5W.

Deflection-Address Gates. This structure is made in annular cone sections and consists of a grounded metal piece with eight metal plates mounted around it in the form of a ring. The structure is precision-mounted to have its center axis aligned with the axis of the gun and the deflection system. The design requirements for the address gates are: (1) the width of each gate plate must exceed five beam widths; (2) the separation between two adjacent gates should be about one beam width (these restrictions ensure a fast pulse rise-time and a pulse width of ~0.5 ns at the target, as required in the program); (3) the coupling between gates should be minimized by using ground planes between adjacent plates; and (4) the capacitance of each gate should be kept to less than ~5 pF in order to facilitate the loading of 4-ns input data pulses. A picture of the fabricated gate structure is shown in Figure 10. In testing the gate structure, some perturbations were observed in the circular rotation pattern of the electron beam (viewed at the target position) when the electron beam scanned a circle through the gates. However, when the rotation pattern was photographed at the exit of the gate structure, most of the perturbations were absent. The corresponding rotation patterns are shown in Figure 11. The problem was due to misalignment of the gate structure relative to the center axis of the electron gun and the conical deflection system. Rebuilding the gate structure improved the rotation pattern but did not eliminate the perturbations. However, with the signal processor tube developed under NRTC's IR&D program, a circular rotation pattern through the gates with little distortion was observed. This tube was therefore substituted for the final deliverable multiplexer device.

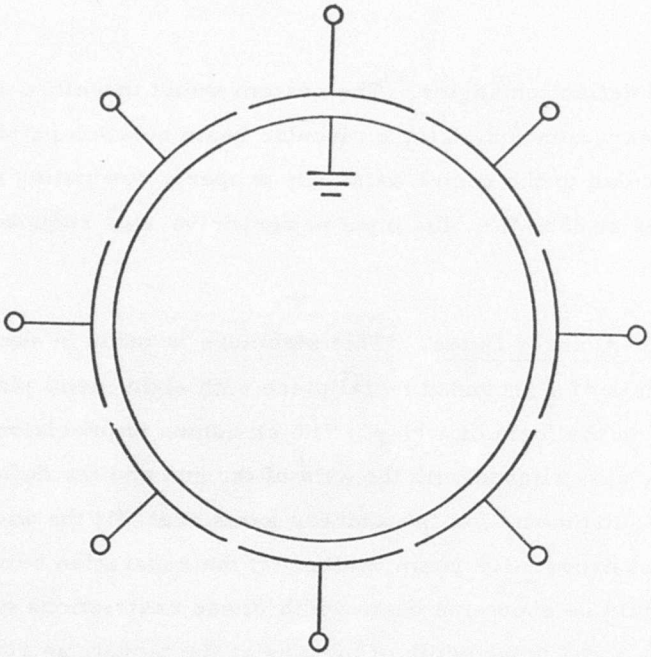

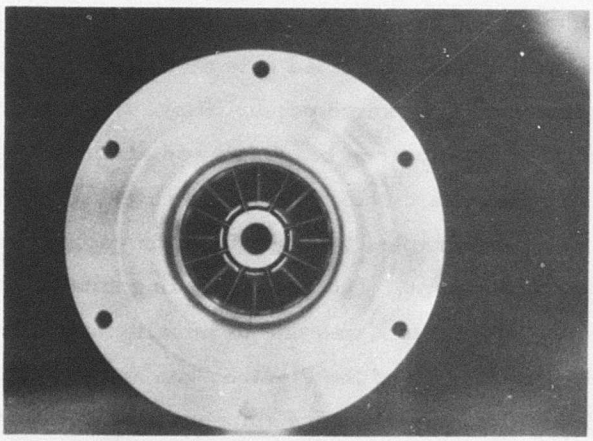

Figure 10. Top: Schematic of the gate structure

Bottom: The gate assembly mounted inside the tube.

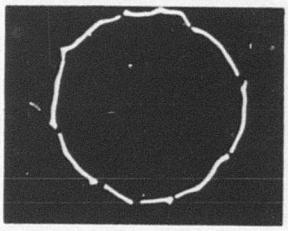

Figure 11(a) Circular rotation through the gate structure observed at the target position.

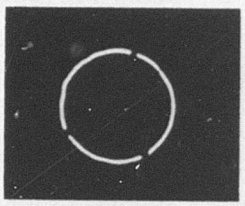

Figure 11(b) Circular rotation pattern observed as the beam emerges from the gate structure.

Einzel Lens. The Einzel lens is a three-aperture or a three-cylinder strong lens. Its function in the multiplexer is to bend and focus the conically-rotating beam onto the target. The lens should be designed for very low spherical aberration and its center axis should be exactly aligned with the axis of the processor. If the beam rotation pattern is elliptic rather than circular, the beam cannot be focused onto the target from all azimuthal positions. Similar results will follow with even perfect conical beam rotation if the lens is misaligned, and especially so if the lens exhibits large spherical aberration. The latter becomes worse as one moves away from the center of the lens. Hence, to reduce aberration problems, the lens radius must be made about twice the radius of beam rotation where the beam enters the lens. Also, the theoretical results of El-Kareh et al.,[7] may be used to design a lens with low spherical aberration. A lens fabricated on their results showed good focusing characteristics.

Funnel. This device is used to ease the alignment requirements on the target. The function of the funnel is to position and center the electron beam, after it is bent by the Einzel lens, onto the target.

Consider a three-cylinder Einzel lens. If one cylinder is removed and a flat plate perpendicular to the cylinder axis is inserted in place of it, a funnel-like device results. The design of this device is now similar to the design of a unipotential lens. Figure 12 shows the funnel and target assembly.

Target Heat Sink and Phosphor Screen. In order to ensure that the electron beam generates a circular rotation pattern before the beam is focused by the Einzel lens onto the target, it became necessary to incorporate a phosphor screen in the target heat sink assembly. This permits viewing the beam rotation pattern and subsequently making any necessary adjustments to optimize the rotation pattern. The phosphor screen was made on a donut-shaped glass disk. The phosphor side vacuum seals against the tube envelope by a viton O-ring, and the bottom side seals against the target heat sink. Figure 12 shows a drawing of the assembly, and photographs of the screen-heat sink unit are shown in Figure 13.

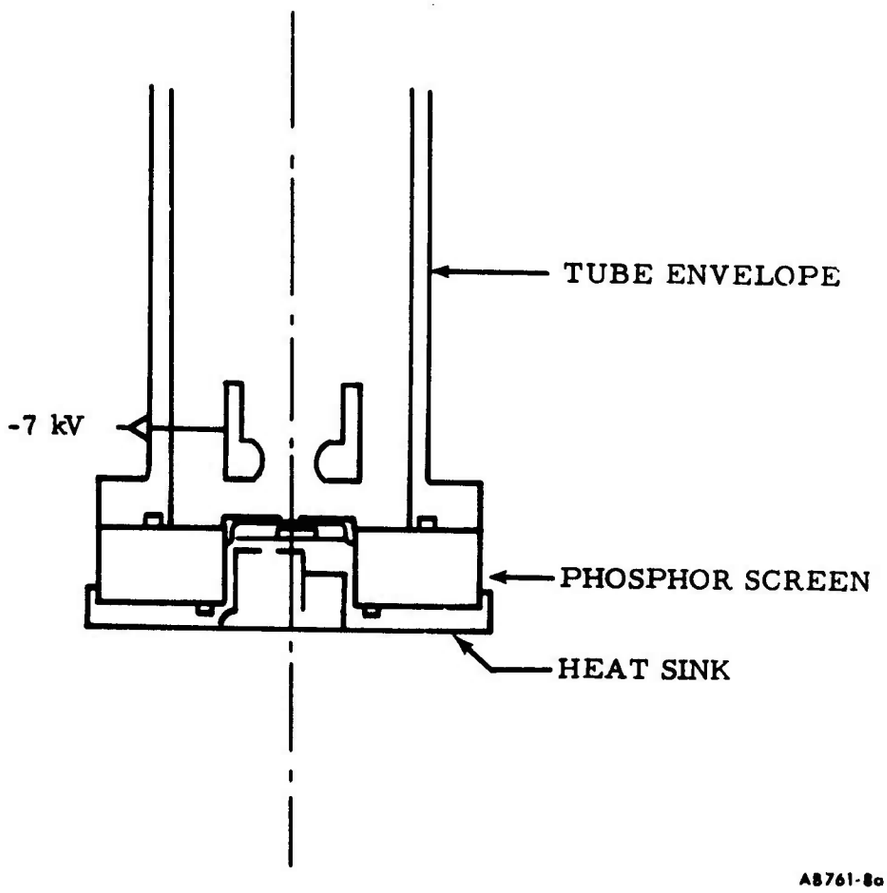

Figure 12. Schematic of the funnel and target assembly.

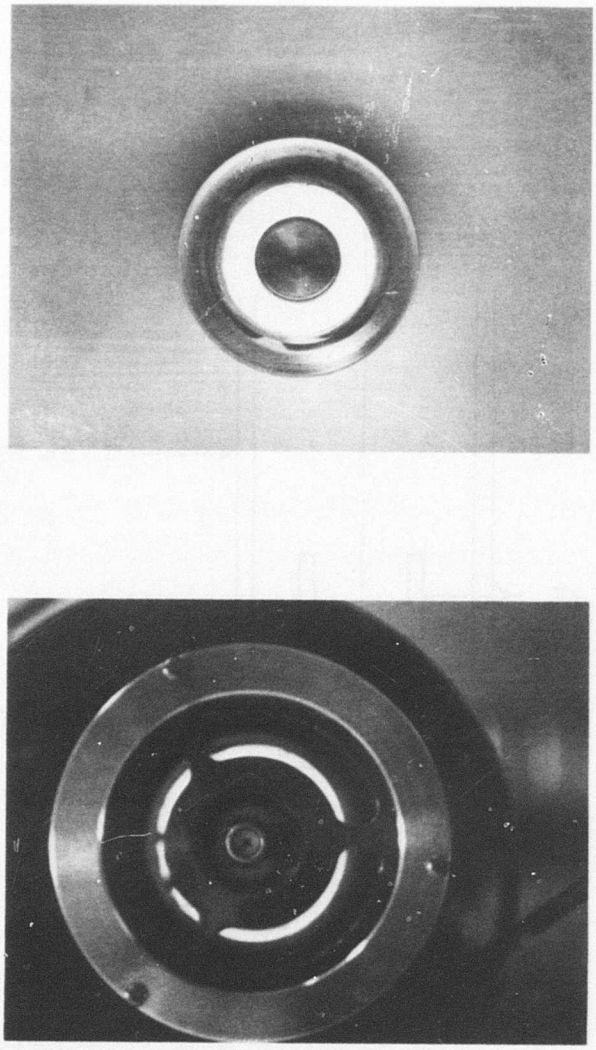

Figure 13. Target heat sink and phosphor screen assembly.

Top: The bright region is the phosphor screen. The hole in the center is the target position.

Bottom: A view from the tube end with the beam in circular rotation.

Tube Envelope. The multiplexer tube is built in standard 1.5-inch stainless steel tubing, except the Einzel lens where a larger diameter envelope is used. Figure 14 shows a schematic of the tube, and a picture of the assembled tube is shown in Figure 15. Inputs to the tube include: 5 for the electron gun at -10 kV; 3 for the deflection system; 8 gates; 1 for the Einzel lens at ~-6 kV; and 1 for the funnel at ~-6 kV. The target assembly includes a heat sink, phosphor screen, O-ring flange, dc bias connector and a 50Ω broadband vacuum feedthrough.

3.4 BROADBAND OUTPUT DC LEVEL ADJUSTMENT

The program specifications require a variable output dc level between 0V and -5V. Conceptually, this can be achieved in the scheme shown in Figure 16. If the 50Ω load termination is isolated from ground by a variable 5V power supply, the program objective will be realized. On the other hand, if a grounded termination should be required, the variable dc level could be provided through a 500Ω resistor, as shown in Figure 3-13(c). However, at -5V output dc level, the power dissipated in the 500Ω resistor will be 5W. Since a broadband 500Ω resistor with this power rating is not available, a different technique had to be used.

In order to supply dc level variation on a broadband transmission line, a 50Ω stripline on alumina substrate was fabricated with standard OSM-type terminal connectors. The dc connection to the stripline was provided inductively in order to prevent coupling of high frequency digital signals from the stripline to the dc input. Figure 17 shows a schematic of the circuit and the completed unit.

The transmission response of the unit was measured from 100 MHz to 4 GHz using an HP8410A network analyzer, an HP8690A sweep oscillator, and an HP 8740 transmission test-unit. Some narrow resonance was observed between 3 and 3.6 GHz. The transmission coefficient was better than 0.95 over

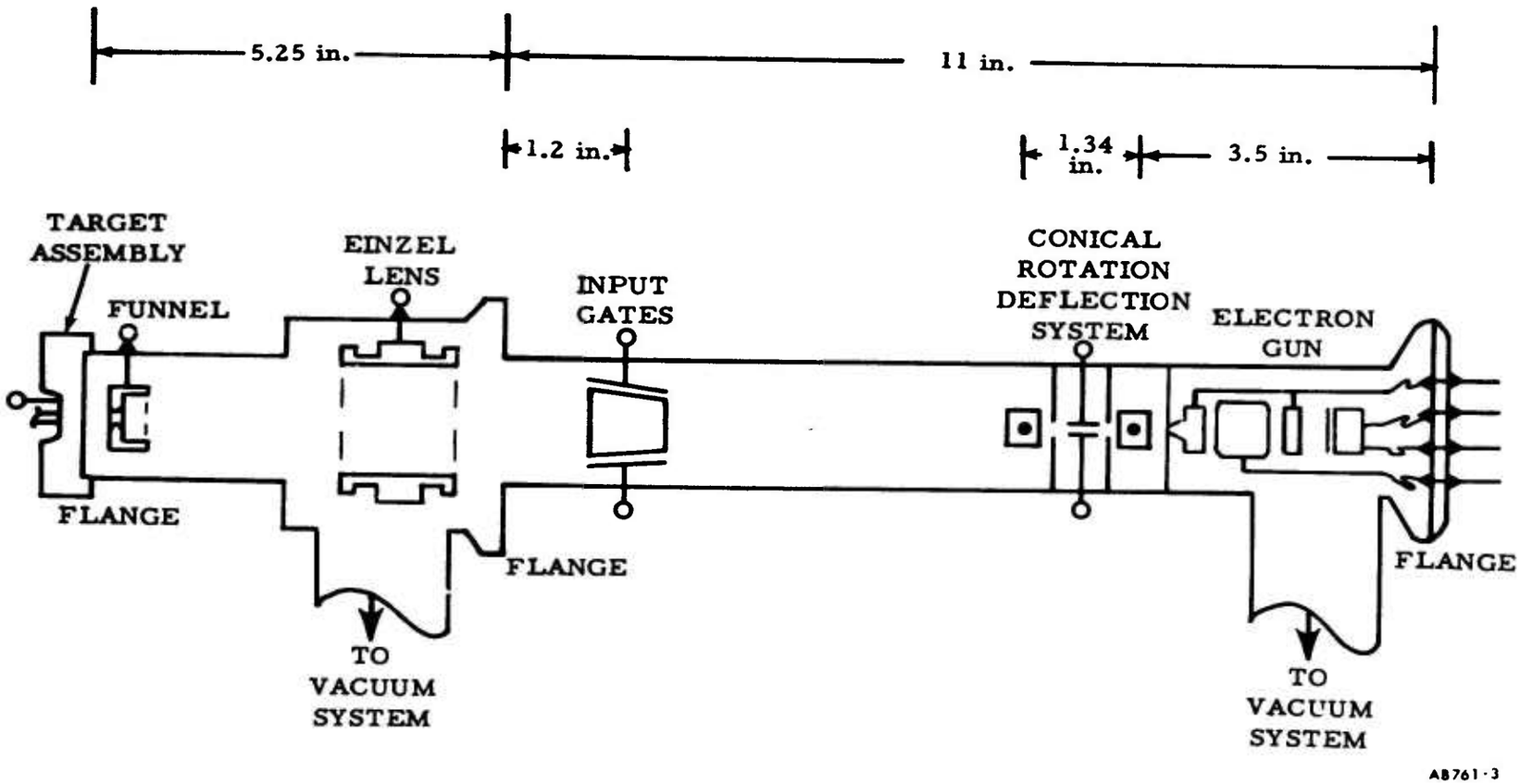

Figure 14. A schematic cross-section of the EBS multiplexer tube. The tube housing is in 1-1/2 inch stainless steel tubing. The Einzel lens housing ID is 2.15 inches.

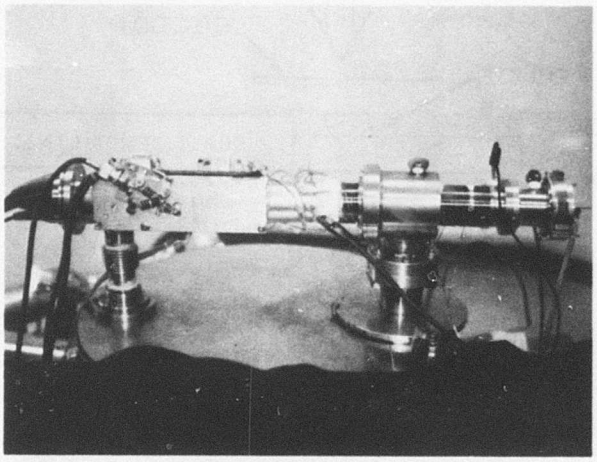

Figure 15. Multiplexer tube mounted for testing.

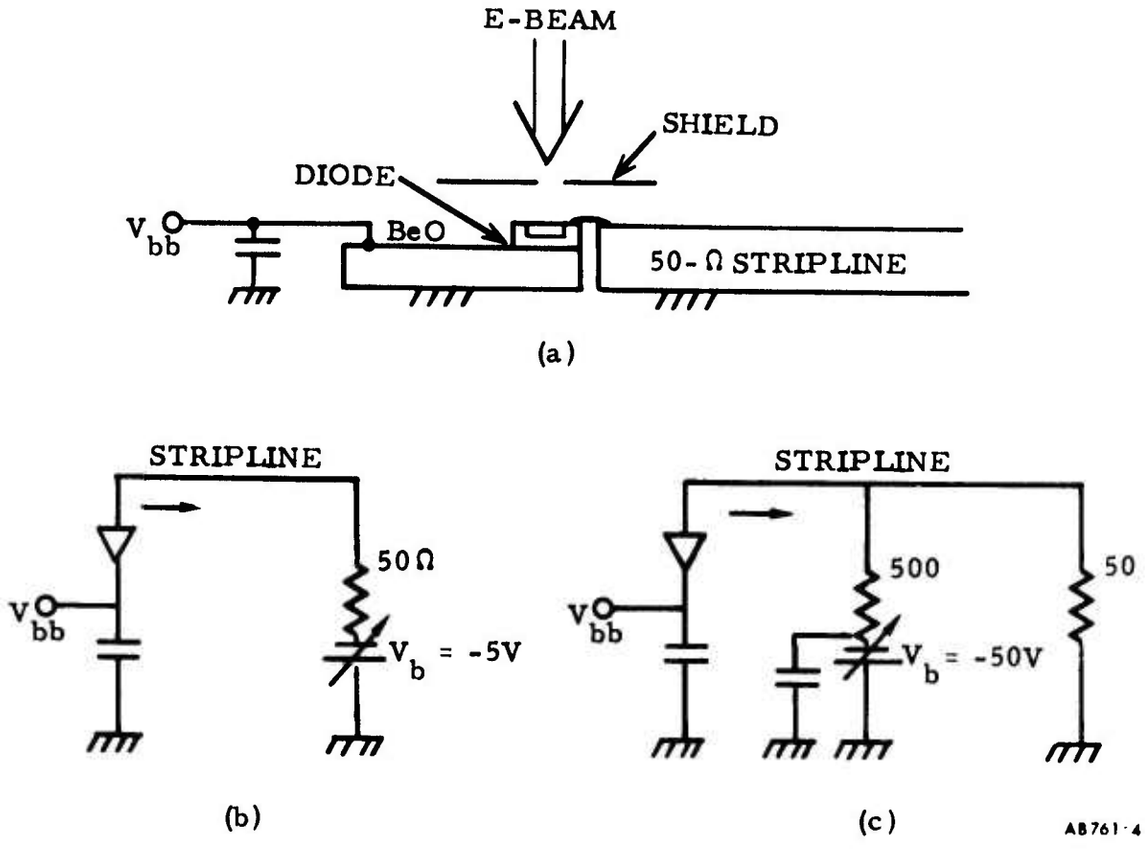

Figure 16. Target mount and biasing scheme: positive output current.

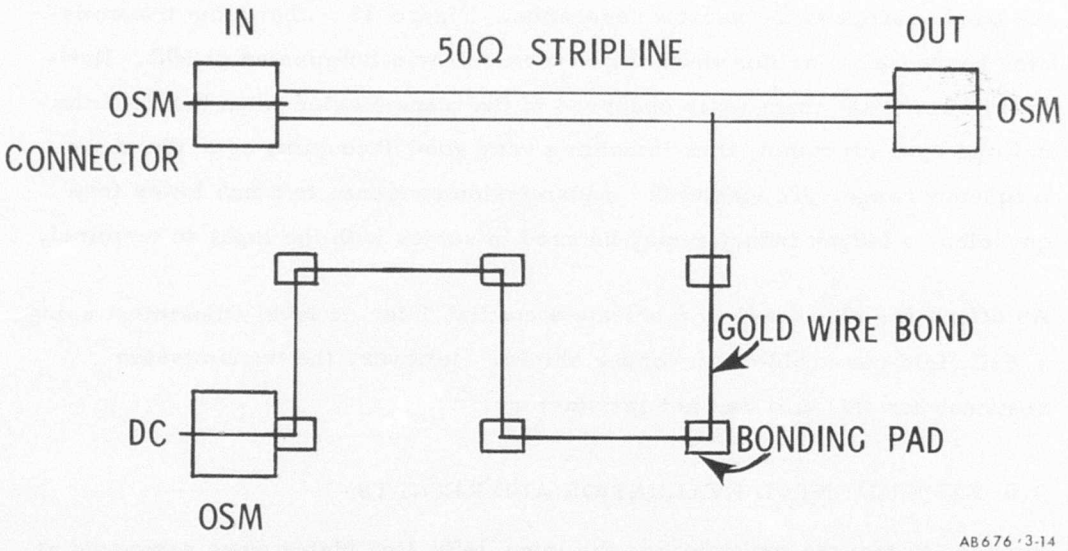

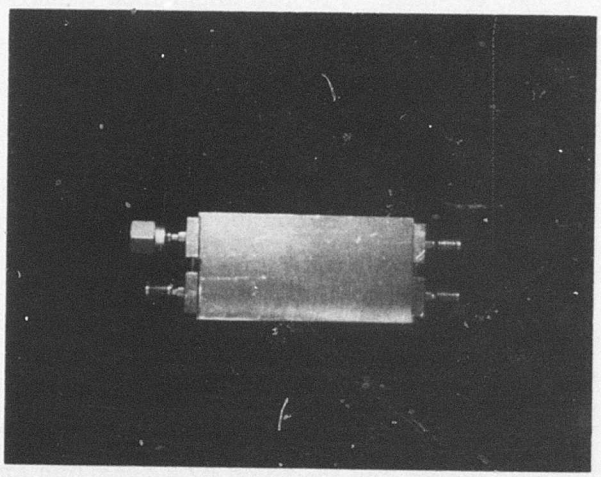

Figure 17. Top: Circuit for output variable dc level control. The stripline is made on alumina substrate.

Bottom: Fabricated unit.

the band, except at the narrow resonance. Figure 18 shows the transmission response. For this test, the dc terminal was terminated at 50Ω. However, very little change was observed in the transmission when the dc terminal was open circuited, thus indicating very good decoupling over the above frequency range. To extend the transmission response to much lower frequencies, a larger inductor may be used in series with the input dc terminal.

An effort was also made to fabricate a coaxial T for dc level adjustment using a 50Ω rigid coax cable with copper shield. However, the transmission response for this unit was not satisfactory.

3.5 EXPERIMENTAL EVALUATION AND RESULTS

In order to test the multiplexer, the input deflection plates were resonated at about 250 MHz. Series inductive resonance with 10Ω line termination was used. The 10Ω impedance level was chosen in order to increase the Q of the resonant circuit. A narrow-band 50 to 10Ω impedance transformer was used at each input for matched line terminations. This technique reduced the input power required for all three pairs of deflection plates to less than 5W in spite of a large deflection amplitude (0.7 cm radius at the gates). The circuit for each pair of deflection plates was tuned for nearly zero line reflection using an HP8410A network analyzer in conjunction with an HP8690A sweep oscillator and an HP8741A reflection test unit.

The driver for the deflection system was a homemade narrow-band class C transistor amplifier. Figure 19 shows a block-diagram schematic of the power division for the deflection system. Phase shift between the vertical and horizontal deflection plates was provided by a coax line and an additional resonant circuit for fine tuning. The vertical deflection plates must be driven 90° out of phase with respect to the horizontal plates. In addition, signal delay should be introduced in the vertical plates for electron beam travel time from the horizontal deflection plates to the vertical plates.

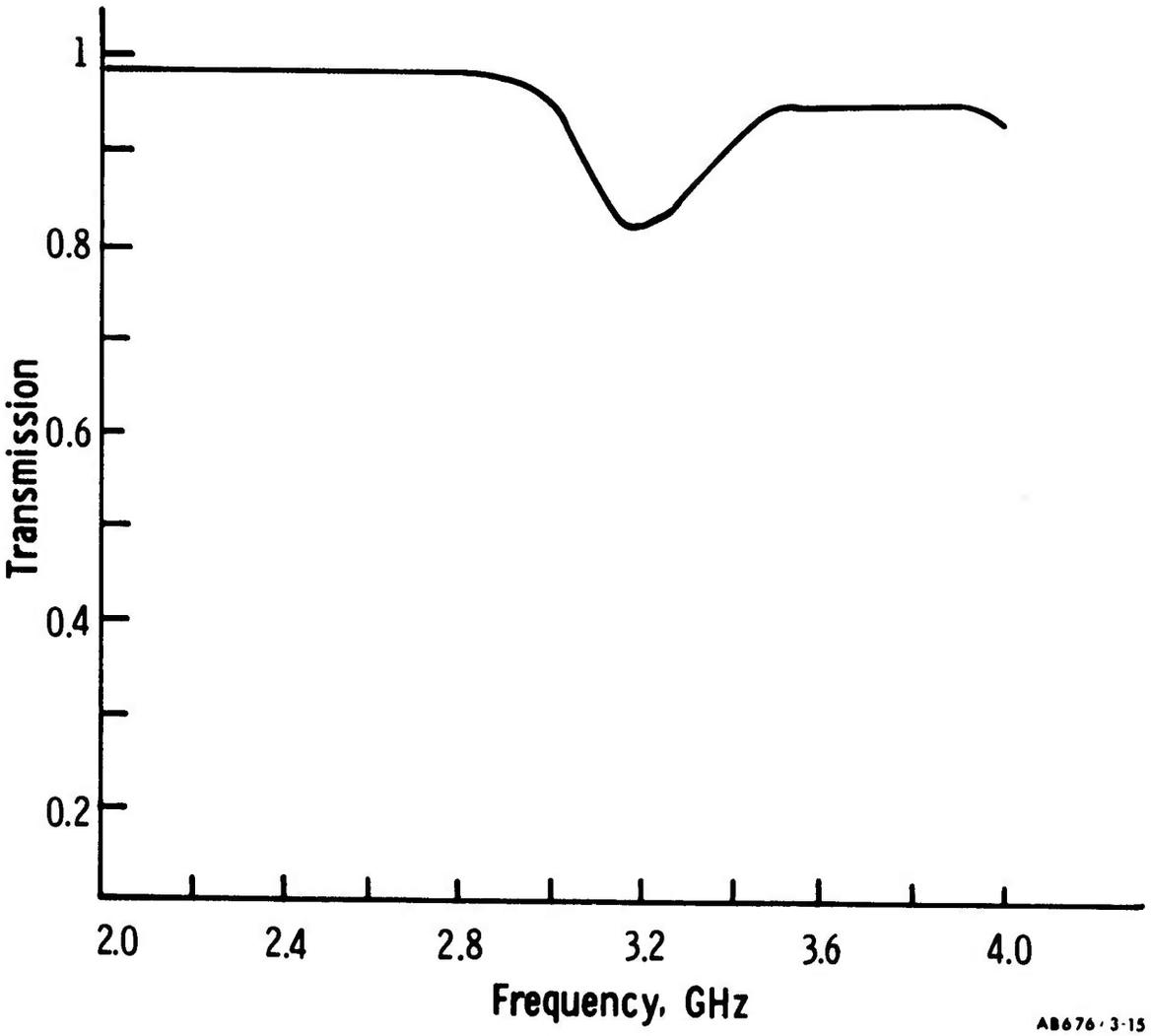

Figure 18. Transmission response of the dc-level adjuster. The response from 0.1 to 2 GHz was essentially flat at 0.98.

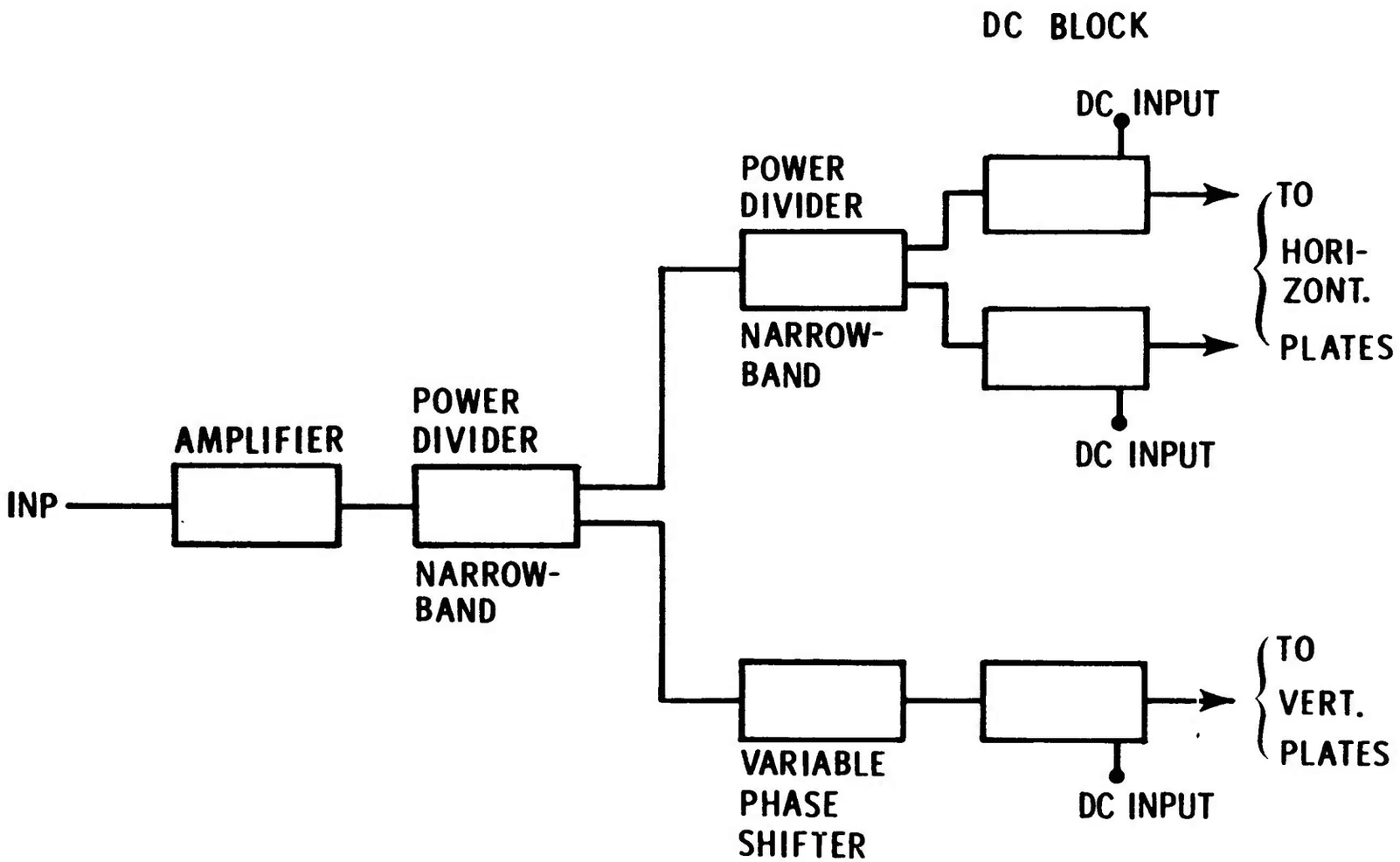

Figure 19. Block diagram schematic of power division for the deflection system.

The high-voltage bias to the gun was derived from a single supply. Independent supplies were used for the funnel and Einzel lens.

Testing of the tube showed the output to be extremely sensitive to the Einzel lens voltage and to the changes in the phase and amplitude of the deflection-system input signal. Operation of all the gates was demonstrated. However, one gate produced 50% less signal than others. The signal level corresponding to this gate could be increased by making small changes in the rotation pattern, or by rotating the target, or slightly moving the beam position. However, these changes resulted in a decrease of the signal level corresponding to another gate.

A small magnet was mounted on the envelope of the target assembly. By rotating the magnet about the target, the beam position at the target could be changed slightly. This provided a means of aligning and of fine-tuning the beam relative to the target and resulted in obtaining fairly uniform ouput signal for the seven gates which were completely operational.

Figures 20 and 21 show some of the output data patterns. Up to 7V output signal was demonstrated. However, at this level the signal amplitudes corresponding to the different gates were quite unequal. At a signal level of ~5V, the amplitudes were fairly equal.

The pulse rise-time was in the range of 0.2 - 0.3 ns. That is, the target output pulse waveform for some gates had a higher rise-time than for others. The output pulse is generated by using an input signal on a gate to deflect the beam onto or off the target. Hence, a variation in the output pulse rise-time is expected if the beam travel time from off to on is not the same for all the gates.

The gate voltages needed for producing an output pulse were in the range 12 - 17V dc for all the gates, both negative and positive. It was necessary to bias most of the gates negative in order to have the electron beam strike the

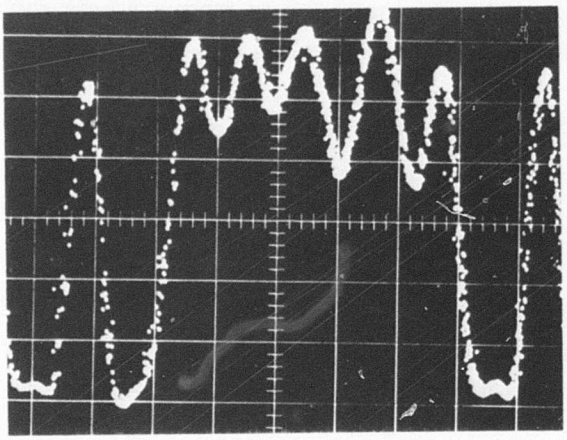

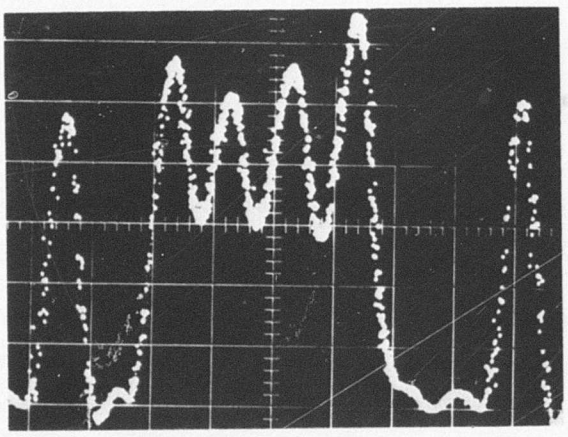

Figure 20. Output data patterns. Vertical, 1V/div. Horizontal, 0.5 ns/div.

Top: 1-0-1-1-1-1-1-0-1
Bottom: 1-0-1-1-1-1-1-0-0-1

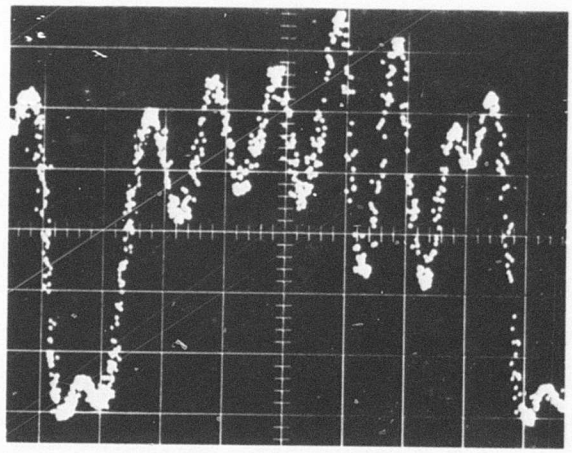

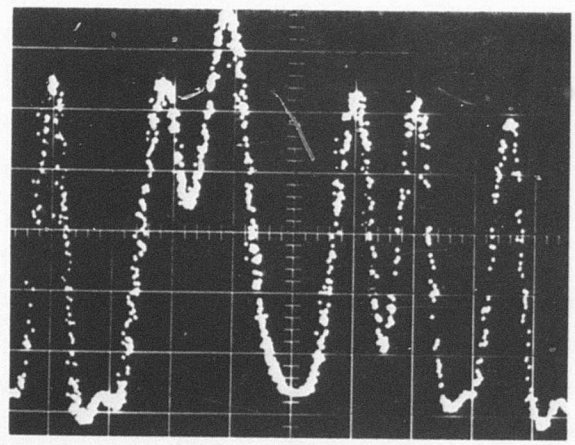

Figure 21. Output data patterns. Vertical 1V/div., Horizontal, 0.5 ns/div.

Top: 0-1-1-1-1-1-1-1-0
Bottom: 1-0-1-1-0-1 1-0-1

target from each gate position with Einzel lens and funnel voltages set at their operating points. In addition, the bias level was not the same for all the gates. These variations in gate bias and input signal levels arise if the gate structure and the target are misaligned or if the beam rotation pattern distorts when the beam is focused onto the target. We have, in fact, observed distortions in the beam rotation pattern as the beam is bent and focused by the Einzel lens closer and closer to the target. (See Figure 2 for a schematic of the electron beam trajectory.) This effect was reduced by moving the target about 1.5 in. farther away from the lens. The complete elimination of distortion is difficult and requires a lens design with very little spherical aberration and low sensitivity to variations in electron trajectory. However, if such a design were incorporated, the electron trajectory from the Einzel lens to the target would become insensitive to variations in gate voltage, and consequently exceedingly high gate voltages would be needed at the gates.

In order to determine the dynamic behavior of gates, one gate was driven with a variable pulse generator having 50Ω load impedance. A 50Ω termination was used at the gate input. In the experiment the beam was dc deflected by the X-Y deflection plates through the above mentioned gate, and the Einzel lens was biased to deflect the beam to the target. The gate pulsewidth varied from 4 to 20 ns, and the gate voltaged needed to produce the full output signal was 20V, as compared to 17V if a dc voltage was used at the gate. The pulse generator signal rise-time was 1 ns, but the target output showed less than 1 ns rise-time. Figure 22 shows the target output waveform. The pulse generator output showed some ringing due to an imperfect termination, and this appears in the target output as well.

The sensitivity of the multiplexer output to variations in the input voltages was measured. The change in an input voltage that would produce a 50% change in the output is given below. Only one input voltage was changed at a time.

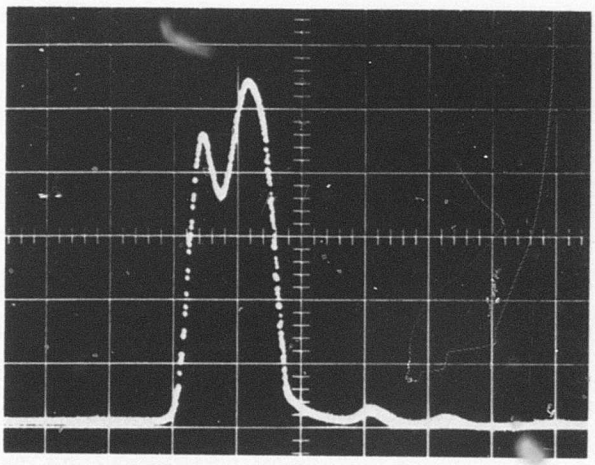

Figure 22. Target response to a single 4 ns pulse on an input gate. Vertical, 1V/div. Horizontal, 2 ns/div.

Electron Gun Voltage:	±50V at -10 kV
Gun Focus Voltage:	±150V at -9.3 kV
Einzel Lens Voltage:	±35V at 5.5 kV
Funnel Voltage:	+50 at 7 kV -20
X-Y Deflection Plates Voltage:	±7V

The voltage settings on the Einzel lens and funnel need not be fixed at the above values and could be changed. For example, the lens voltage could be increased and the funnel voltage decreased. The above results indicate that very stable power supplies are needed for the multiplexer operation.

Some 60-Hz modulation of the electron beam has been observed. A high-voltage RC filter was built into the gun supply circuit. This resulted in a reduction of the 60-Hz modulation. However, breakdowns in the gun produced some large transients from the RC filter, causing a large instantaneous surge in gun current and consequently diode failure. The filter was therefore removed. The 60-Hz modulation was later found to be caused by pickup through the Kovar ceramic input terminals. Magnetic shielding by Mu-metal and the use of filters reduced the modulation significantly.

SECTION IV

MULTIPLE-GUN, SINGLE-TARGET MULTIPLEXER

4.1 TUBE DESIGN AND FABRICATION

The technical effort in this part of the program was mainly aimed at demonstrating the feasibility of our device concept presented in Section 2.3. To this end, it was not necessary to build a complete 8-gun multiplexer. In addition, an optimized 8-gun device could not be fabricated within the time period and funds available to this phase of the program.

The multiple-gun, single-target approach offers several advantages as compared to the single-gun design, and this task of the program was carried out with the goal of demonstrating these advantages, which include:

1. Each input gate operates on a separate electron source. After being addressed, each electron beam is centered by individual x-y deflection plates at the target. This virtually eliminates the alignment problems encountered in the single-gun multiplexer.
2. A shorter tube is feasible.
3. A phosphor screen will not be required at the target. This makes the heat sinking more efficient and may allow output signal levels to 7V.
4. The shorter tube should allow for a better focused beam spot, and hence high current density.
5. Due to a shorter tube length and rather relaxed alignment requirements, tube fabrication is easier and more economical.
6. The design is well compatible with cold cathodes with the potential of making a compact, low-power device realizable. However, any work on cold cathodes was beyond the scope of this program.

The disadvantage of the design is the need for extra dc and RF power to operate several guns. (However, if reliable cold-cathode sources become available, the power consumption will be greatly reduced.) In addition, all the guns need to have fairly similar electron emission characteristics. However, by providing independent grid and anode bias control for each gun, the beam currents from the guns can be equalized.

As described in Section 2.3, the target output pulse is generated by sinusoidally deflecting the electron beam from each gun across the target. The electron beam strikes the target for a short time period in each RF cycle. This time period defines the output pulse width; the output rise-time will be a function of the beam RF deflection amplitude and the beam width (see Section 4.2).

For sin ωt deflection, where ω is the frequency in radian/sec, one output pulse is obtained per sinewave period when the electron beam strikes the target at the deflection maximum (or minimum), i.e.,

$$\omega t = (2n+1)\pi/2, \quad n = 0, \pm 1, \pm 2, \ldots$$

On the other hand, if the electron beam coincides with the target at the point of zero RF deflection ($\omega t = n\pi$, $n = 0, \pm 1, \pm 2, \ldots$), two output pulses are obtained per sinewave period. Hence, two bits can be generated per electron gun. In order to be able to utilize this higher bit rate, it will be necessary to switch each input gate between two incoming data lines once during each RF period. In this manner, each input gate continuously samples the information on two incoming data lines. A 2-bit multiplexer or a fast double-pole switch may be used for this purpose.

As an example, for 2 Gbits/sec output data rate and a 4-gun tube, the deflection frequency is 250 MHz, eight input lines each carrying 250 Mbits/sec data may be used, and each input gate has to sample two data lines in each 4 ns RF period. Hence, the sample time per input data line is 2 ns.

In the design and fabrication of the multiple-gun digital multiplexer, emphasis was placed on simplicity, ease of fabrication, and reduction in device size and pulse amplitude required for the input gates. The various components are briefly described below.

Electron Gun. Various guns were tested to check their power consumption and beam current capabilities. A short gun type SEW114K produced up to 140 mA target current. However, the electron emission was unstable at this level. The gun operated at a filament power rating of 0.3A at 6.3V. Our initial design concept was to use four of these guns for a 4-gun multiplexer. A 2.3-inch OD tube was needed for this design.

In later work, a small 3-gun array mounted on a single stem type VT31C was obtained commercially. The three guns are well aligned, require a single 6.3V, 0.9A current drive, and can be easily mounted in 1.5-inch tubing. When testing the array, the guns produced sufficient electron current to meet the program requirements. Due to the small size of the array, rigid construction, low power consumption, ready commercial availability, and low cost, it was decided to build a 3-gun multiplexer in a 1.5-inch diameter stainless steel envelope.

Using the 3M machinable glass, a 12-pin high-voltage mount was fabricated for the gun. This provides separate grid and anode voltage control for each gun in the array. In addition, the gun mount allows easy and fast replacement of the 3-gun array should the replacement be necessary. Figure 23 shows the gun and its glass mount as well as the fabricated tube envelope.

Tube Envelope. A schematic of the final tube is shown in Figure 24. The tube housing is in standard 1.5-inch OD stainless steel tubing and is about 25 cm long. Approximately 2.5 cm of the tube is used for the gun-array glass base. The tube could therefore be shortened by this amount if the commercial glass base were eliminated prior to mounting the gun array. However, in the interest of ease of gun replacement, we decided not to

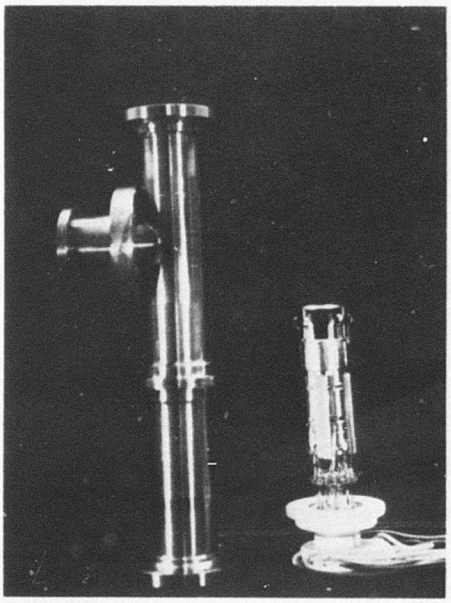

Figure 23. The multiplexer tube envelope and the 3-gun array mounted on in-house made glass feed-through.

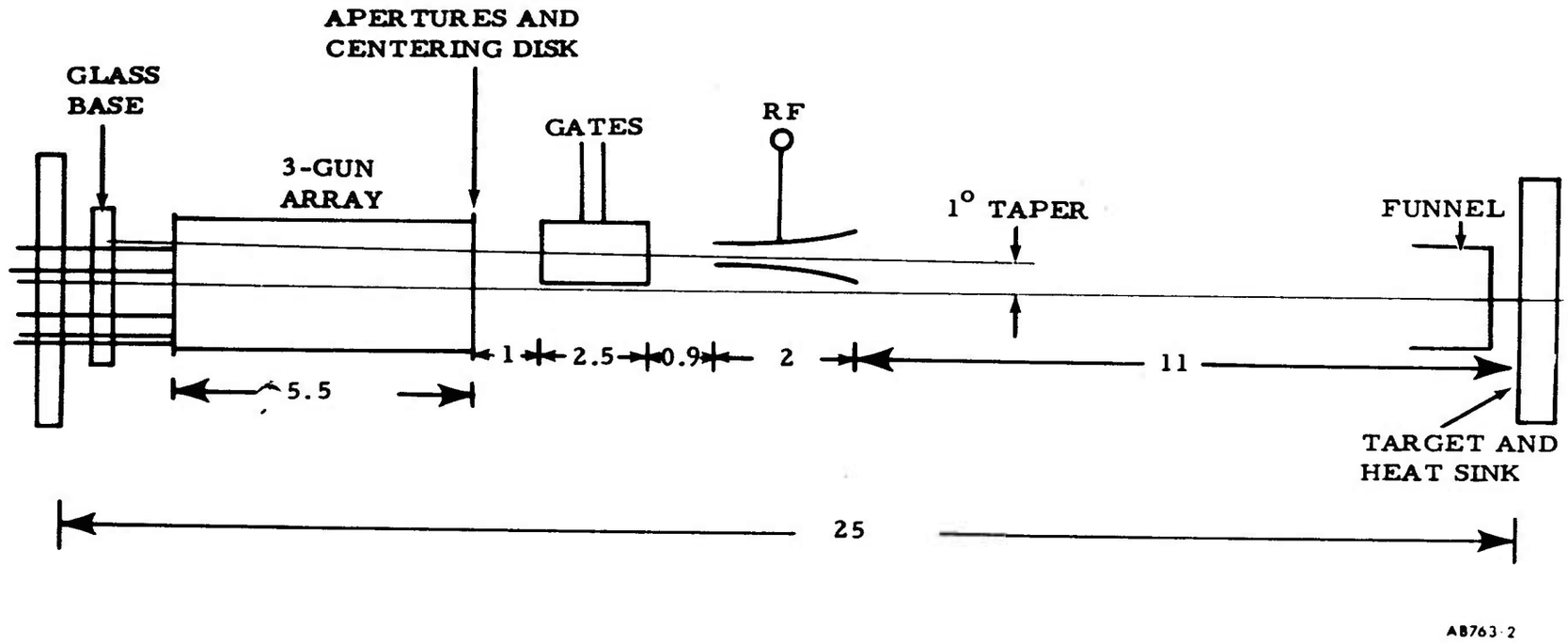

Figure 24. Schematic of the 3-gun multiplexer. The deflection plates for only one gun are shown. The dimensions are in centimeters.

include the 2.5 cm shortening. The remaining length of the tube was decided with the goal of keeping the required input gate signal below 10V. In addition, the beam deflection angle should be kept to a few degrees in order to prevent excessive elongation of the beam spot size in the direction perpendicular to the deflection axis. (Elongation of the spot reduces the beam current density and, consequently, the target output.) The capacitance of the input gate is also an important consideration, since very fast input data are to be used at the input.

Input Gates and RF Deflection Plates. The deflection voltage needed to produce a deflection amplitude x by a pair of electrostatic deflection plates is given by

$$V = \frac{2a \times V_B}{Lb}$$

where V_B is the beam voltage, a is the gap on the deflection plates, b is the length of the deflection plates, and L is the field-free distance to the target. The input gate signal is required to deflect the beam by at least one beam diameter in order to change the logic state of the multiplexer output. Assuming a beam width of 0.1 cm, b = 2 cm, V_B = 10 kV, and L ≃ 15 cm, we obtain a gate voltage of V_G = 10V.

For the above dimensions, the beam deflection angle is about 3.4 degrees. If the length of the gate deflection plate is increased to 2.5 cm, V_G will be reduced to 8.5V and the deflection angle will increase to about 3.7 degrees. The electron guns in the array have a ~1-degree convergence angle. Therefore, the actual deflection angle will be less than 3 degrees and should not cause excessive elongation of the beam.

The electron transit time through the deflection plates determines the pulse and RF response. Assuming a ramp gate signal,

$$V_G(t) = V_o\, t/\tau \qquad t \leq \tau$$

$$= V_o \qquad t \geq \tau$$

the deflection response can be computed by calculating the electron velocity as it leaves the deflection plates. The equation of motion is

$$m \frac{d^2x}{dt^2} = -e \frac{V(t)}{a}$$

Denoting the electron transit time through the plates by T, we have

$$\frac{dx}{dt} = -\frac{e}{m} \int_o^t \frac{V(t)}{a} \qquad t \leq T$$

$$\frac{dx}{dt} = -\frac{e}{m} \int_{t-T}^t \frac{V(t)}{a} \qquad T \leq t \leq \tau$$

or

$$v_x = -\frac{e}{2m} \frac{V_o}{a\tau} t^2 \qquad t \leq T$$

$$v_x = \frac{eV_o}{2ma\tau} (2tT - T^2) \qquad T < t \leq \tau$$

For $T \leq t < \tau + T$, the initial electron velocity within the plates should be taken into account. From this analysis, it can be shown that for a ramp input with rise time τ, the (0-100%) deflection rise time is $\tau + T$. If τ is 2 ns, a value of $T \leq 0.5$ ns will provide a rise time of ~2.5 ns or less. Figure 25 shows the y- and x-axis deflections for optimum phase angle between the gate signal and the RF deflection signal.

The transit time through the plates is $T = b/v$, where for 10 kV electrons $v = 6 \times 10^9$ cm/sec. For b = 2.5 cm, T is 0.42 ns. The capacitance of the deflection plates is ~1.5 pF. Fringing-field and feed-through capacitance should add 1 to 2 pF. The RC rise time with 50Ω shunt impedance is about 0.3 ns and is quite reasonable for data rates to 400 Mbits/sec.

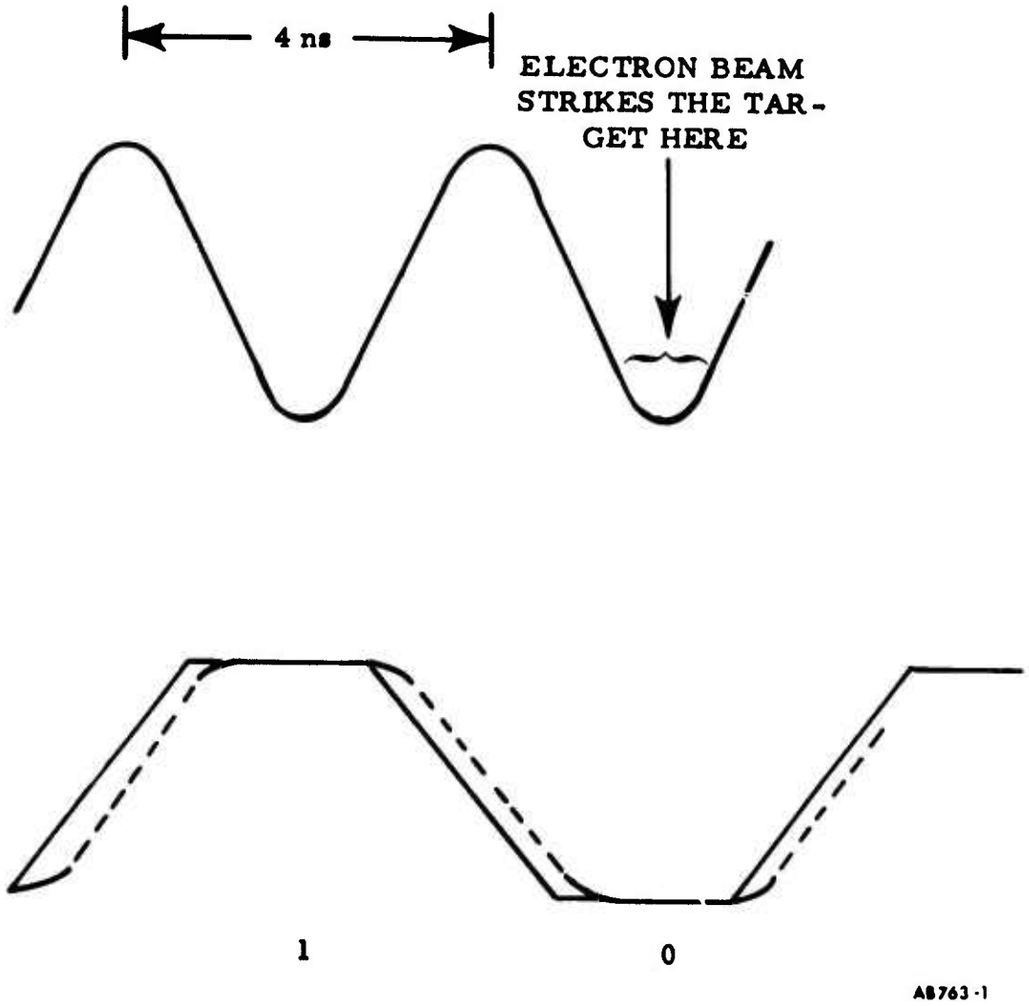

Figure 25. The gate and RF deflection amplitudes. A 1-0, 250-Mbits/sec input-data pattern is assumed at the gate input. The dashed lines represent the beam deflection amplitude.

For the RF deflection plates, the transit angle should satisfy the condition

$$\omega T \leq 1$$

Using 2-cm long deflection plates, T will be about 0.33 ns for 10 keV electrons. Hence, the deflection frequency can be as high as $1/2\pi T = 500$ MHz. The RF deflection plates were initially resonated for operation at 260 MHz.

Target Mount and Heat Sink. The target diode was mounted on a gold-metallized BeO chip. The chip thickness was less than 10 mils. Connection to the output 50Ω connector was provided by directly bonding from the diode contact pad to the connector gold-metallized center pin. This mounting technique achieved very low series inductance and was also used for the single-gun multiplexer. Figure 26 shows the BeO target assembly mounted on a copper heat sink. A phosphor screen was not required for the multiple-gun design.

4.2 ANALYSIS OF THE TARGET OUTPUT

In our multiple-gun, single-target design, the electron beam excitation striking the EBS target is generated by sinusoidally deflecting a pencil beam across the semiconductor target. The electron beam pulse arriving at the target is therefore time-dependent and its pulse shape is a function of the oscillation frequency as well as the beam spot size. The pulse shape was calculated from a simple geometrical model as described below.

Two modes of operation are possible: (1) the electron beam is centered on the target at the point of its maximum deflection (i.e., $\omega t \simeq (2n+1)\,\pi/2$); (2) the electron beam strikes the target at the point of zero RF deflection amplitude (i.e., $\omega t = 0, \pm n\pi$).

Figure 27 shows the deflection of a spot beam of radius R_2 across a circular EBS diode of radius R_1. The cross-hatched area is the portion of the beam contributing to the diode output current. The area is given by

BY-PASS CAPACITOR

OUTPUT
CONNECTOR

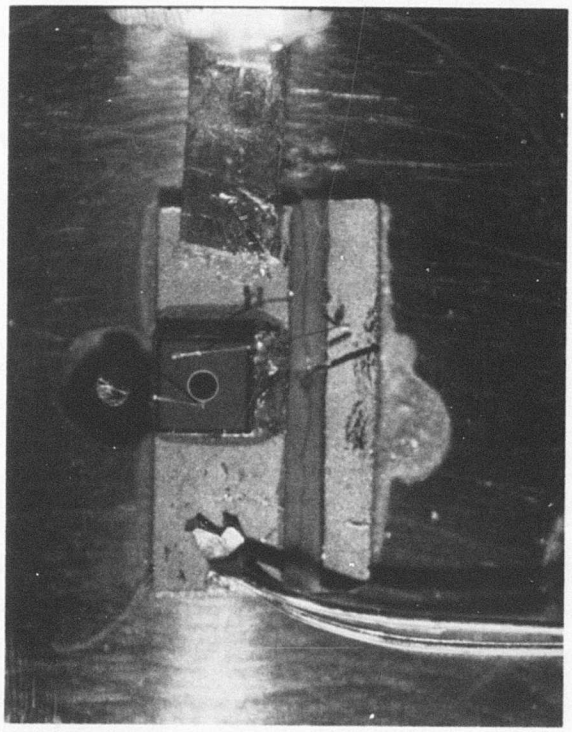

DC BIAS

Figure 26. The multiplexer target die-attached to a BeO chip and soldered to a heat sink.

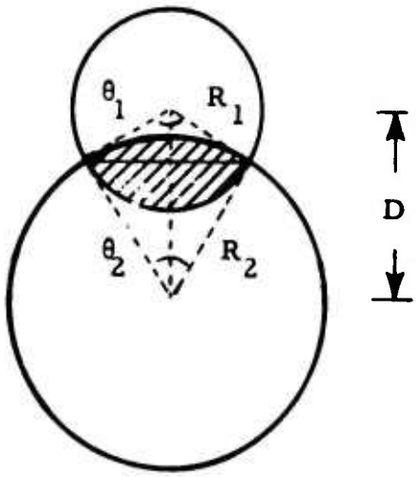

Figure 27. An electron beam of radius R_2 being deflected across an EBS target of radius R_1.

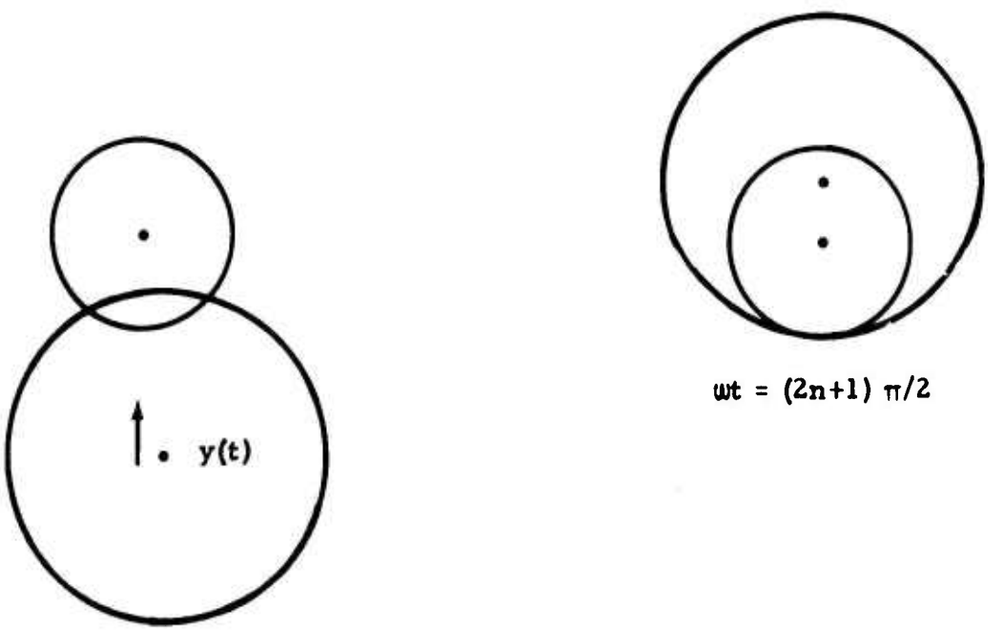

AB763-3

Figure 28. The beam position relative to the EBS target for sinusoidal deflection at $\omega t = (2n+1)\,\pi/2$, n=0, 1, 2....., and at an intermediate time.

$$A = \frac{R_1^2}{2}(\theta_1 - \sin\theta_1) + \frac{R_2^2}{2}(\theta_2 - \sin\theta_2) \tag{4-1}$$

Denoting the distance between the centers of the two circles by D, θ_1 and θ_2 are obtained from the following

$$R_2 \sin\frac{\theta_2}{2} = R_1 \sin\frac{\theta_1}{2} \tag{4-2}$$

$$R_2 \cos\frac{\theta_2}{2} + R_1 \cos\frac{\theta_1}{2} = D \tag{4-3}$$

The distance D and angles θ_1 and θ_2 vary with time as the beam sweeps the target. From Eqs. (4-1) - (4-3), we have

$$\frac{A}{\pi R_1^2} = \frac{1}{2\pi}\left[\theta_1 + \left(\frac{R_2}{R_1}\right)^2 \theta_2\right] - \frac{D}{\pi R_1}\sin\frac{\theta_1}{2} \tag{4-4}$$

where

$$\theta_1 = 2\cos^{-1}\left[\frac{1 + \left(\frac{D}{R_1}\right)^2 - \left(\frac{R_2}{R_1}\right)^2}{2\frac{D}{R_1}}\right] \tag{4-5}$$

Figure 28 shows the beam position relative to the target position at the point of maximum deflection and at an intermediate time. Denoting the beam deflection amplitude by y(t),

$$y(t) = y_o \sin\omega t \tag{4-6}$$

the distance D is given by

$$D(t) = y_o - y_o \sin\omega t - (R_2 - R_1) \tag{4-7}$$

Using Eqs. (4-4) - (4-7), the electron beam pulse striking the target was calculated for various beam diameters and deflection amplitudes assuming a beam of constant current density. The results are shown in Figures 29 and 30. The pulse width can be obtained from Figure 29. For example, for y_o = 10 mm and R_2 = 0.5 mm, the pulse width is $\omega\Delta t = 0.9 = 2\pi\Delta t/T$, where T is the sinewave period. At 250 MHz, T is 4 ns, and we find $\Delta t \sim 0.6$ ns. If the beam radius is reduced to 0.25 mm, $\omega\Delta t$ becomes ~0.5 for y_o = 10 mm, and the pulse width becomes ~0.3 ns. Also note that the rise-time increases as the deflection amplitude, y, decreases.

For the case when the electron beam coincides with the target at zero RF deflection (i.e., $\omega t = 0$), the electron beam pulse shape is given in Figures 31 and 32. A much narrower pulse width results in this case and the beam deflection amplitude must be reduced in order to increase the pulse width to near 0.5 ns. However, the smaller amplitude also results in higher rise-times, which is not desirable. For y_o = 2.5 mm and R_2 = 0.5 mm, $\omega\Delta t$ is ~0.4 ns and Δt is ~0.26 ns at 250 MHz RF deflection. The 0 - 100% rise-time corresponds to $\omega\Delta t_r = 0.15$, or $\Delta t_r \sim 0.1$ ns. These results therefore indicate that for the case when the beam strikes the target near the point of zero RF deflection, the pulse width may be too narrow and the pulse rise-time too long. On the other hand, since two bits can be obtained in an RF (sinewave) period, the concept is quite appealing.

Finally, it should be added here that in the above calculation the beam current density has been assumbed constant across its cross section, whereas the current density is usually a Gaussian function. The Gaussian profile should result in a smaller rise-time and narrower pulse width as compared to the values calculated above.

Both of the above modes of operation were evaluated experimentally during the testing of the multiplexer tube.

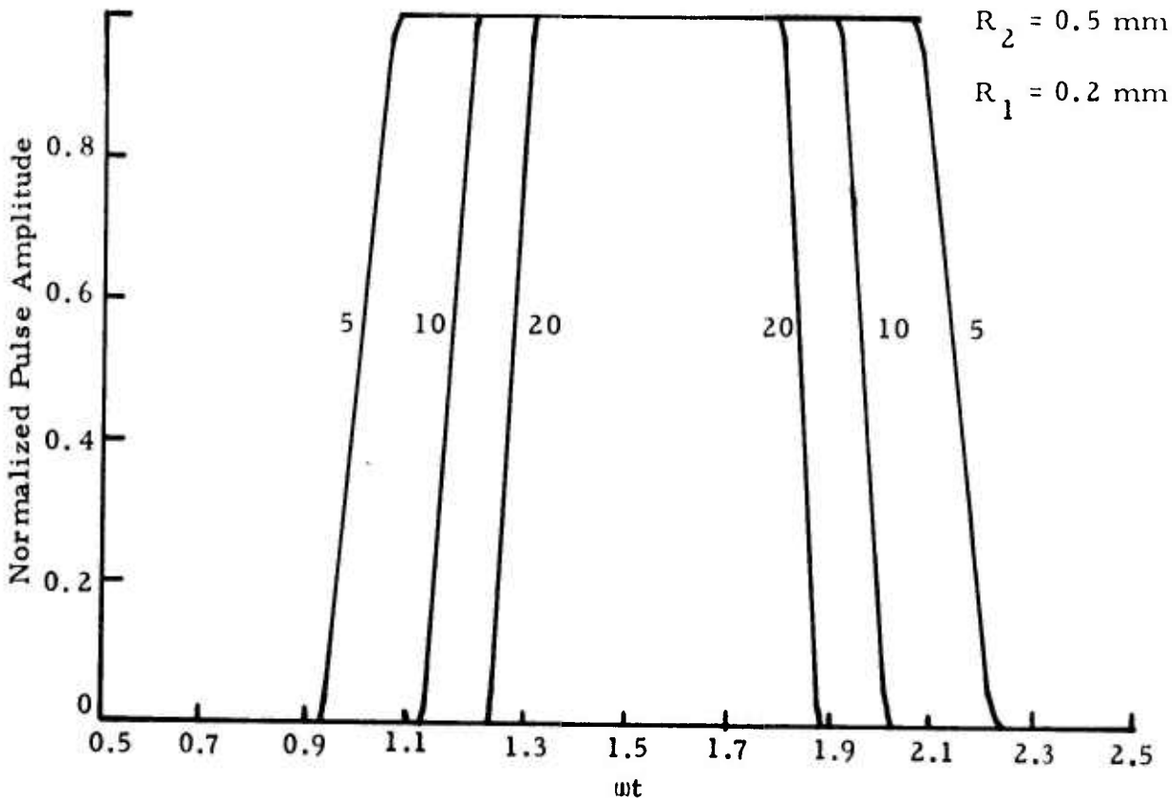

Figure 29. The electron beam pulse striking the target when a beam of radius R_2 is sinusoidally deflected across an EBS target of radius R_1. The beam center coincides with the target center near $\omega t = \pi/2$. The beam deflection amplitude (in millimeters) is used as a parameter.

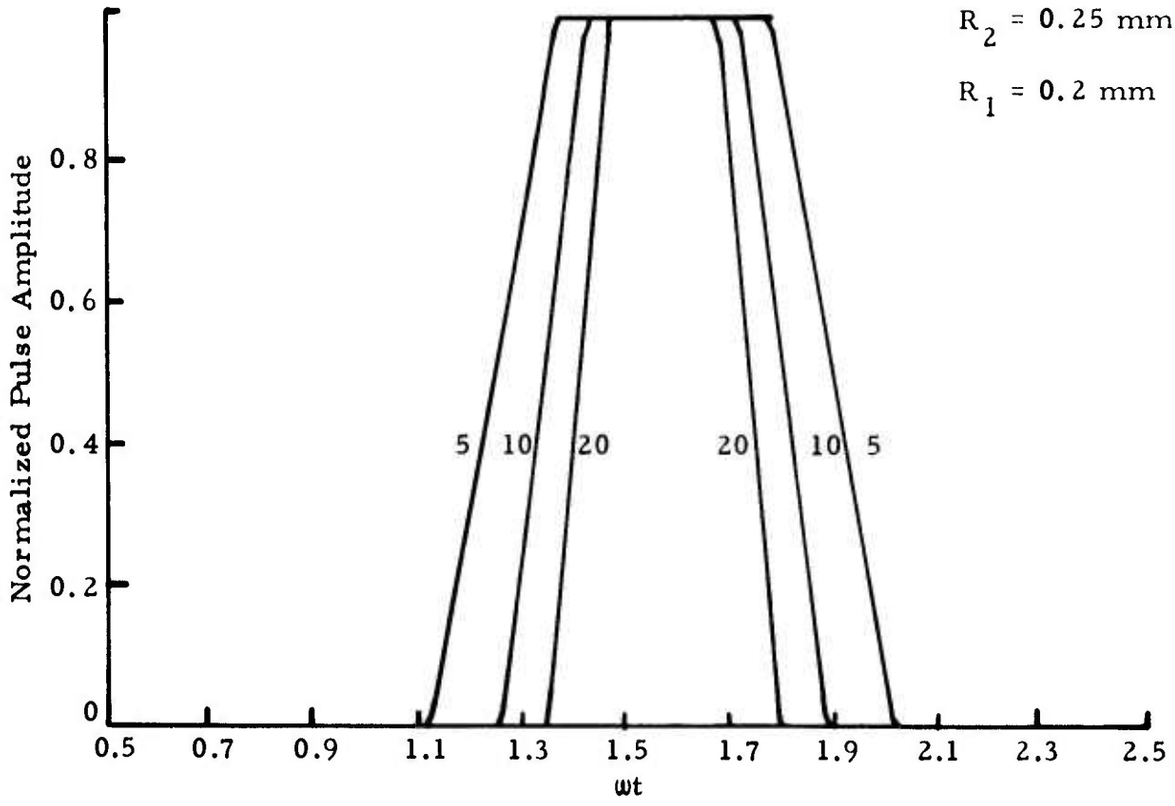

Figure 30. The electron beam pulse striking the target when a beam of radius R_2 is sinusoidally deflected across an EBS target of radius R_1. The beam center coincides with the target center near $\omega t = \pi/2$. The beam deflection amplitude (in millimeters) is used as a parameter.

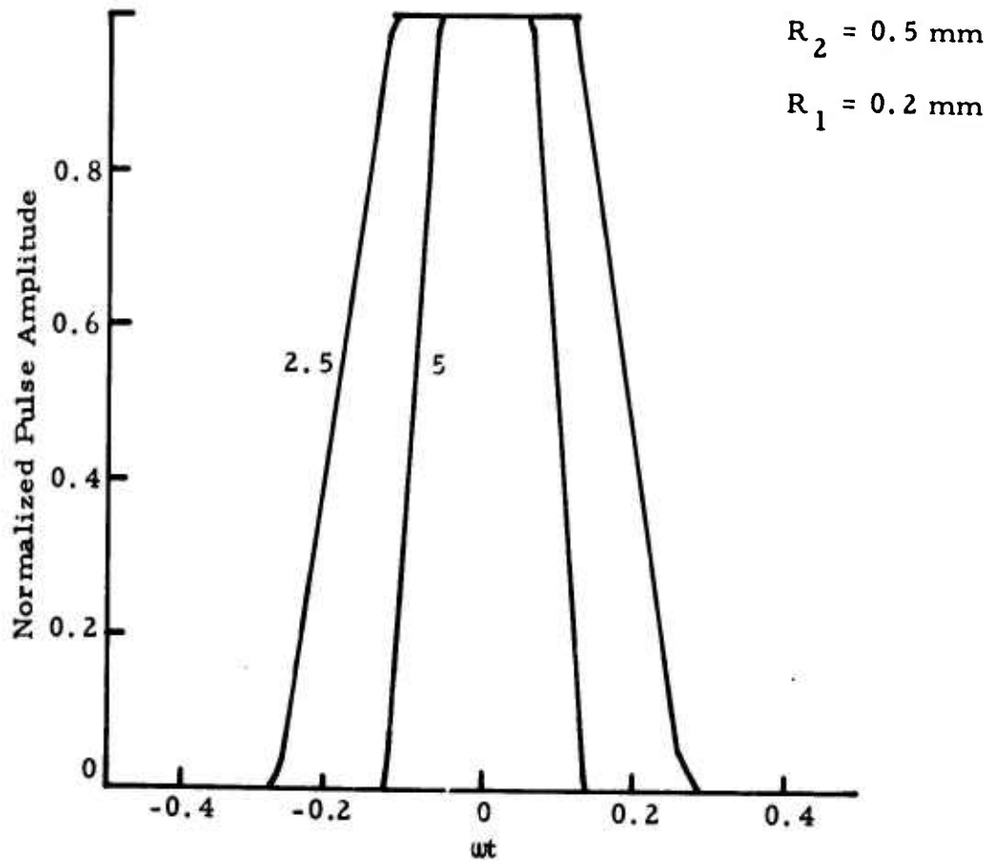

Figure 31. The electron beam pulse striking the target when a beam of radius R_2 is sinusoidally deflected across an EBS target of radius R_1. The beam center coincides with the target center at $\omega t = 0$. The beam deflection amplitude (in millimeters) is used as a parameter.

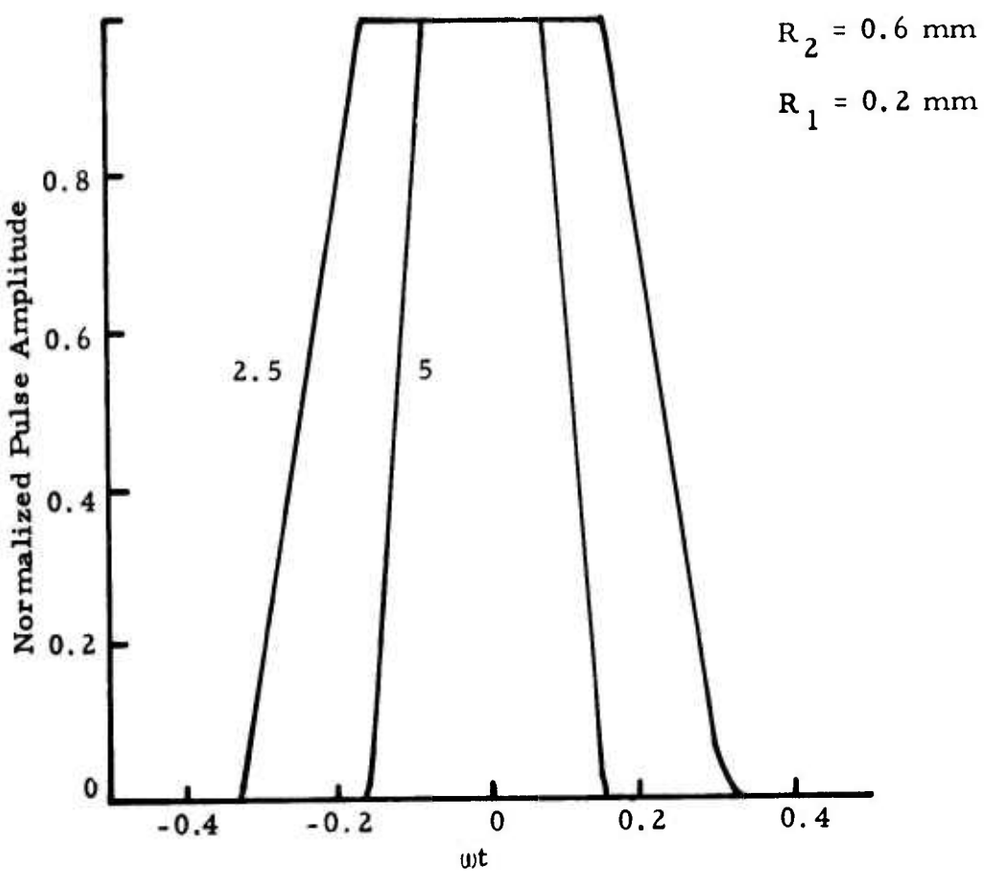

Figure 32. The electron beam pulse striking the target when a beam of radius R_2 is sinusoidally deflected across an EBS target of radius R_1. The beam center coincides with the target center at $\omega t = 0$. The beam deflection amplitude (in millimeters) is used as a parameter.

4.3 EXPERIMENTAL EVALUATION AND RESULTS

After the digital multiplexer was fabricated and assembled, it was mounted on an ion-pump vacuum system for evaluation (see Figure 33). The tube was heated under vacuum to nearly 100°C for one day before the electron guns were activated. The pressure in the vacuum system after bake-out was in the low 10^{-8} Torr range.

The initial test of the multiplexer with a phosphor screen target was successful and showed the proper operation of the device. Independent control and alignment of each electron beam was demonstrated. Figure 34 shows some of the patterns observed on the phosphor screen. The input deflection plates were resonated at 260 MHz for this test.

An EBS target assembly was subsequently mounted on the multiplexer tube, and operation of all three guns was demonstrated. However, the three guns did not generate equal signal amplitudes in the EBS target. In this test, all three guns had common cathode, grid, first anode, and focus electrodes. (The heater filaments were in series.) Therefore, it was not possible to control the electron current in each gun independently. Consequently, non-uniformities in the cathode emission and/or gun structure resulted in the unequal target outputs for the three guns.

In order to be able to control the electron current and the beam spot size from each gun independently, a biasing circuit incorporating high-voltage Zener diodes was built which provided grid and first anode control for each gun separately. (The focus electrodes of the three guns were tied together internally on the array and could not be isolated easily.) A single high-voltage supply was used for biasing all three guns. Using this circuit, nearly equal output signal amplitudes were achieved for all three guns by adjusting the grid and anode voltage of each gun.

As described earlier in this section, two modes of operation are possible. In the first mode, one output pulse is obtained from each gun in each sinewave

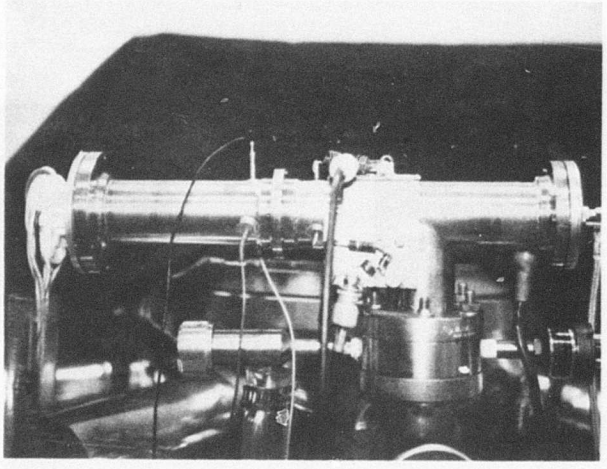

Figure 33. Multiple-gun digital multiplexer mounted on a vacuum system for testing and evaluation.

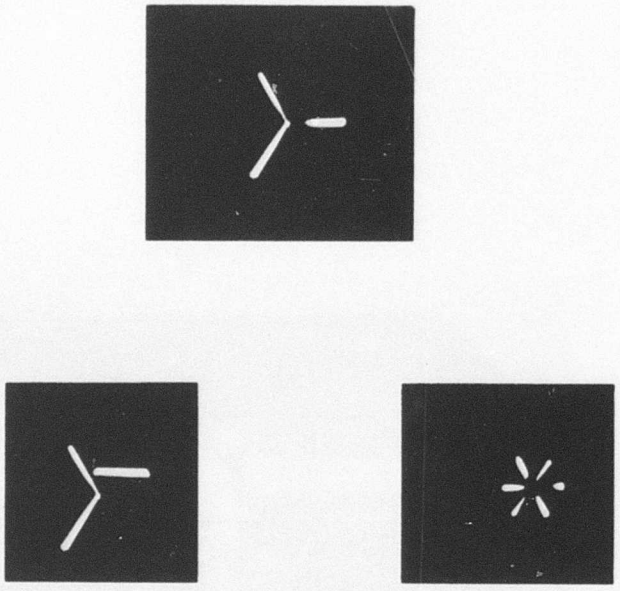

Figure 34. Various patterns obtained on a phosphor screen by deflection modulation of the 3-gun array at 260 MHz. The center of the pattern shows low illumination because the phosphor screen degraded in this region due to excessive electron fluence.

deflection period when the electron beam strikes the target at its maximum RF deflection. On the other hand, two pulses are generated in each RF period when the beam strikes the target at zero RF deflection. Both modes of operation were demonstrated. Initially, the deflection frequency was set at about 260 MHz since we already had amplifiers available at this frequency.

Figures 35 and 36 show the output patterns achieved for the first mode of operation: one pulse per ~4 ns RF period. Up to 7V signal amplitude was demonstrated. The pulse width was variable and could be adjusted by varying the deflection amplitude and/or the spot size. The 10 - 90% pulse rise-time was typically in the range 0.2 - 0.25 ns at 25V diode reverse bias and could be reduced to less than 0.2 ns by increasing the diode bias to 30V. Pulse rise-time was also a function of the deflection amplitude. The output rise-time deteriorated severely when the diode bias was reduced below 20V. The bias dependence of rise-time in the bias range 20 - 30V is due to variation in the electron transit-time in the junction depletion region. As the bias increases, the average junction electric field and the electron velocity increase, resulting in a lower transit-time and hence improved pulse response. At bias levels below 20V, the diode epitaxial region is not totally depleted. Hence, the diode capacitance is higher and the electron velocity is lower, resulting in a poor pulse response, as observed.

The delay between two consecutive pulses in Figure 36 is about 1 ns. This value was arbitrarily chosen to clearly identify the pulse signal from each gun. In actual operation, the delay between two consecutive pulses should be equal to the pulse width.

Figures 37 and 38 show the data patterns for the second mode of operation. Output pulse widths as low as 0.3 ns were achieved in this mode. At lower pulse widths, the output amplitude decreased, indicating frequency response limitations. The pulse width and rise-time were functions of the deflection amplitude as well as the beam spot size.

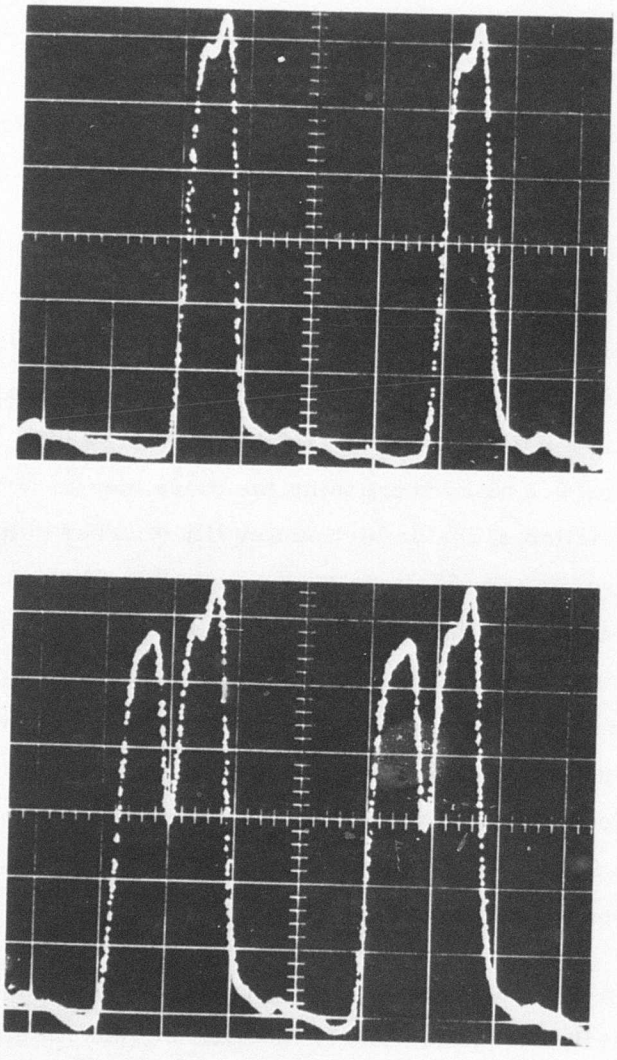

Figure 35. Multiplexer output patterns when one pulse is obtained per gun per RF period:

Top: Output for gun #3

Bottom: Output for guns #2 and #3

Scales: Vertical 1V/div.; Horizontal 1 ns/div.

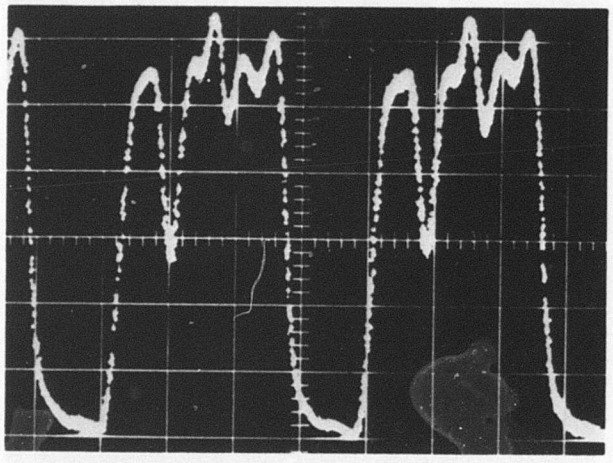

Figure 36. Multiplexer output pattern when one pulse is obtained per gun per RF period: output for guns #1, #2, and #3.

Scales: Vertical 1V/div.; Horizontal 1ns/div.

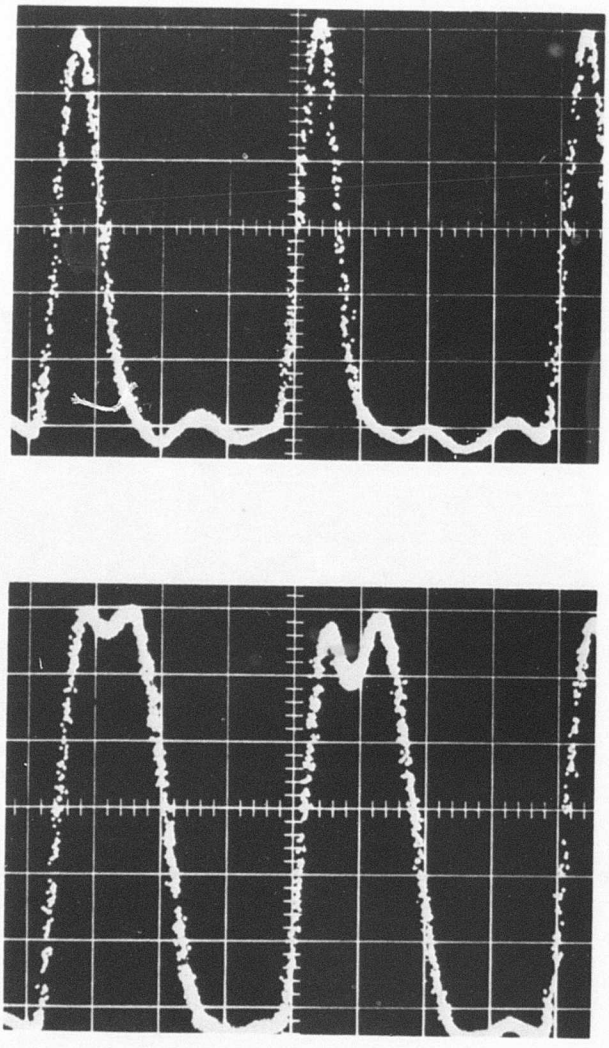

Figure 37. Multiplexer output patterns when two pulses are obtained per gun per RF period.

Top: Pattern for gun #3

Bottom: Pattern for guns #3 and #1

Scales: Vertical, 1V/div.; Horizontal, 0.5 ns/div.

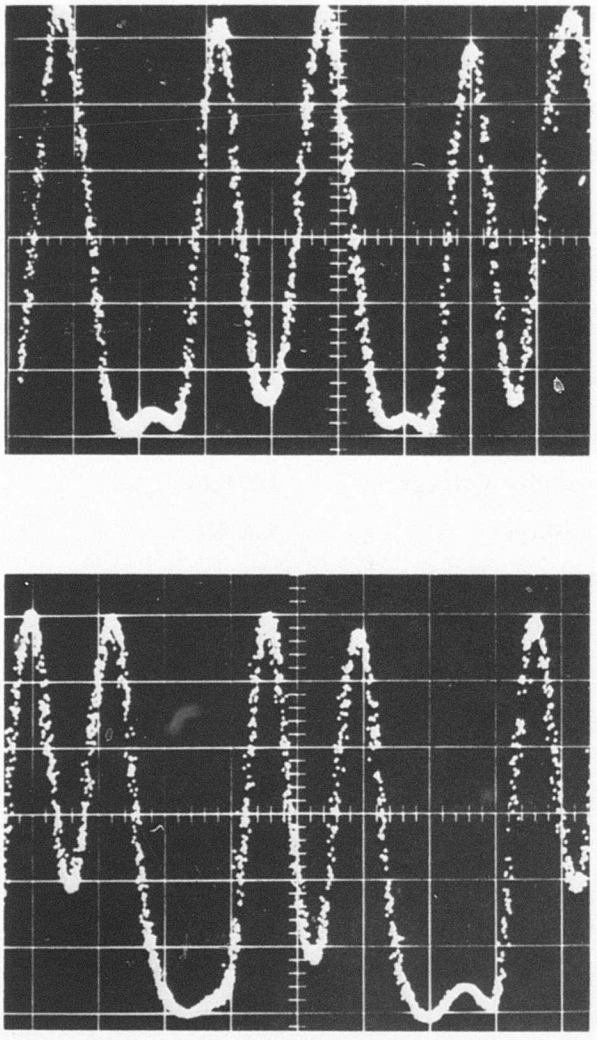

Figure 38. Multiplexer output patterns when two pulses are obtained per gun per RF period.

Top: Patterns for guns #2 and #1

Bottom: Patterns for guns #2 and #3

Scales: Vertical, 1V/div.; Horizontal, 0.5 ns/div.

Since two bits are obtained per gun in each RF period, up to six bits are generated in each period. The delay between two consecutive bits was set at ~0.5 ns and ~1 ns, as shown in the patterns of Figures 37 and 38. The output signal amplitude was typically 6V, and the rise-time was ~0.2 ns. (This mode of operation required less RF power than the first mode.)

The input gate voltage required to change the output logic state (1 to 0 or vice versa) was less than 8V for 10 keV electron beam energy. The input RF power was less than 4W for both modes of operation. The electron gun bias settings for the data in Figures 36 to 38 were:

Filament power	~0.9A at 6.6V
Power supply voltage	-10.5 kV
Focus voltage	-8.6 kV
1st Anode - cathode voltage	150V
Grid - cathode voltage	-10 to 0V
Funnel voltage	-8.2 kV
Input RF power	3.3W

In order to reduce the beam spot size and increase the beam current density at the target, a farily large funnel voltage was used. Without the funnel, the specification of 5V output pulse amplitude could not be achieved.

The results achieved at 250 MHz deflection frequency do not constitute 2 Gbits/sec output data rate. However, the pulse specifications and the data presented do indicate the feasibility of achieving 2 Gbits/sec serial data rate at over 5V signal amplitude. For 2 Gbits/sec data rate, the number of guns or the deflection frequency must be increased. With four guns and operation at 250 MHz, eight bits can be obtained in 4 ns, which is 2 Gbits/sec. Since we have already demonstrated this mode of operation with three guns, extension to four guns is straightforward. It is also possible to achieve 2 Gbits/sec with four guns in the first mode of operation by doing the deflection at 500 MHz. (One bit is obtained per RF period, but since the period is 2 ns, two bits are generated per gun in 4 ns.)

To explore the feasibility of the latter concept, the deflection plates were series resonated at 450 MHz with matched 10Ω line termination (for higher circuit Q). At this frequency, the six watts available from our amplifier did not deflect the electron beam sufficiently to achieve a narrow pulse width and a fast rise-time. Due to the larger power required and the problems associated with operating at high frequencies, this mode of operation does not appear desirable and was not pursued any further. It is much easier to operate at half the frequency and obtain two bits per RF cycle with the beam striking the target at points of zero RF deflection. This mode of operation achieves the highest output data rate with the lowest power consumption at the inputs.

In order to extend the output rate to over 2 Gbits/sec, the input resonance and deflection frequency was changed to 360 MHz (2.8 ns period). For three guns, six bits are obtained in 2.8 ns, which is 2.14 Gbits/sec. Some output data patterns are shown in Figure 39 The input power required was less than 5W.

4.4 TARGET LIFE TEST

An array of four diodes were mounted on a 20-mil BeO chip on a water-cooled copper heat sink. The array was used with a sheet beam electron gun to determine if the diodes could operate at rated power for a long period of time. The sheet beam was operated at 10 kV at a total beam current of 9 mA. Water cooling was used in order to prevent the heat sink temperature from rising above room temperature due to the 90W of power dissipation from the sheet beam.

Initially, one diode failed after bombarding the array with the sheet beam. The failure was probably due to an inadequate metal coverage of the diode poly-silicon slope. After 100 hours at 15 W/mm^2, two diodes failed due to a power supply breakdown. The fourth diode operated to 300 hours at 20 W/mm^2. (The peak rated power in our design was 20 W/mm^2.) The life test was then discontinued and the array was examined to determine the cause of failure in the diodes. Hot spots were observed in the two diodes which

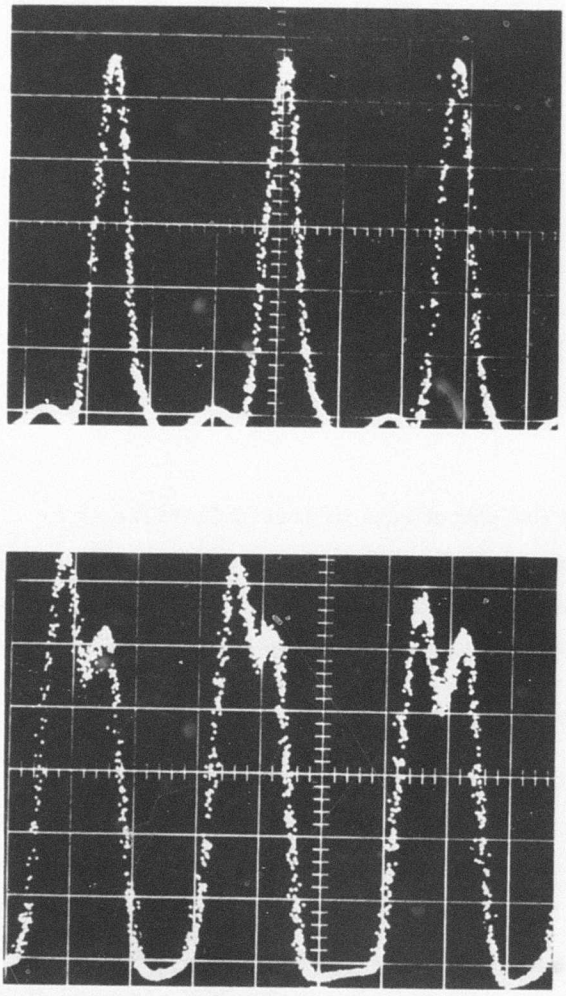

Figure 39. Output data pattern for 360 MHz input deflection frequency.

Top: Pulse output for gun #1, (1-0-0-1-0-0).

Bottom: Output for guns #1 and #2, (1-1-0-1-1-0). The delay between two consecutive bits was set arbitrarily at ~0.3 ns and should be 0.46 ns.

Scales: Vertical, 1V/div.; Horizontal, 0.5 ns/div.

had failed due to the arc in the vacuum system, indicating the failure was due to a sudden increase in power dissipation and device temperature.

Four additional diodes were mounted to continue the life test. The diodes had breakdown voltages over 140V. Operation at 20 W/mm^2 did not create any change in the breakdown voltage during 40 hours of life test. However, the reverse leakage current of one diode increased to 100 μA at 140V bias, still quite small compared to the rated operating current of 100 mA. Unfortunately, due to an operator error, the water valve for the water-cooled heat sink was not opened in the subsequent test. This resulted in an excessively high heat sink temperature due to the power dissipation from the sheet beam. Consequently, all four diodes failed.

The life test results clearly indicate that the target reliability problem in our devices is not one of electron beam-induced radiation damage, but rather a problem of excessive temperatures and insufficient cooling. The target poly-silicon layer and the metal overlay provide an effective shield against the incident electrons, thus preventing radiation-induced damage. By introducing a chromium layer between the silicon surface and the aluminum contact, we have eliminated the failure mode due to Al-Si reaction which occurs at high temperatures. Once operation at rated power is demonstrated for several hours, it is expected that the target will operate indefinitely at this level without failure provided the target temperature does not become too high to cause the formation of localized hot spots.

Thus, by providing a suitable heat sink and sufficient cooling, the stable and reliable operation of the EBS target can be expected, as was demonstrated in our life test.

SECTION V

2-Gbit/sec DIGITAL MULTIPLEXING WITH GaAs TRANSFERRED-ELECTRON DEVICES

The transferred-electron devices (TEDs) operate on the principle of a bulk negative differential mobility that is due to the transfer of electrons from a high-mobility to a low-mobility energy band. So far TEDs have mainly been used for microwave signal generation and amplification. Recently, a new class of high-speed logic elements have been proposed by F. Sterzer.[8] On the basis of those proposals and the experimental data available,[9,10] a parallel-to-serial converter with the potential for 2 Gbit/sec serial data rate is proposed below. The TED multiplexer would be used with a broadband EBS pulse amplifier as a PIN driver.

A schematic of the usual TED logic element is shown in Figure 40. By putting a notch in the device, a notch pulse appears in the output, as shown in the figure. Here the device is biased just below the critical field to sustain a high field domain, and when a negative pulse appears at the input, the high field domain nucleates at the cathode and moves at saturation velocity to the anode, causing a drop in the output current and hence an output pulse.

Now consider two TEDs connected as shown in Figure 41. The input TED is designed to sustain a domain travel time of ~4 ns. A notch of 0.25 - 0.5 ns width is placed at a specific location on the device. The output of the input TED for a 4-ns input pulse is also shown in Figure 41. The output TED is designed for a pulse length of 0.5 ns. With the right bias, when the notch pulse of the input TED reasches the output TED, it launches a domain and a 0.5-ns pulse appears at the output. In this manner, a 4-ns input pulse has been multiplexed to a 0.5-ns output pulse.

Figure 42 shows two input TEDs connected to an output TED to multiplex two lines. The notches in the input TEDs are just 0.5 ns apart to generate two consecutive 0.5-ns pulses at the output for two input pulses. In this

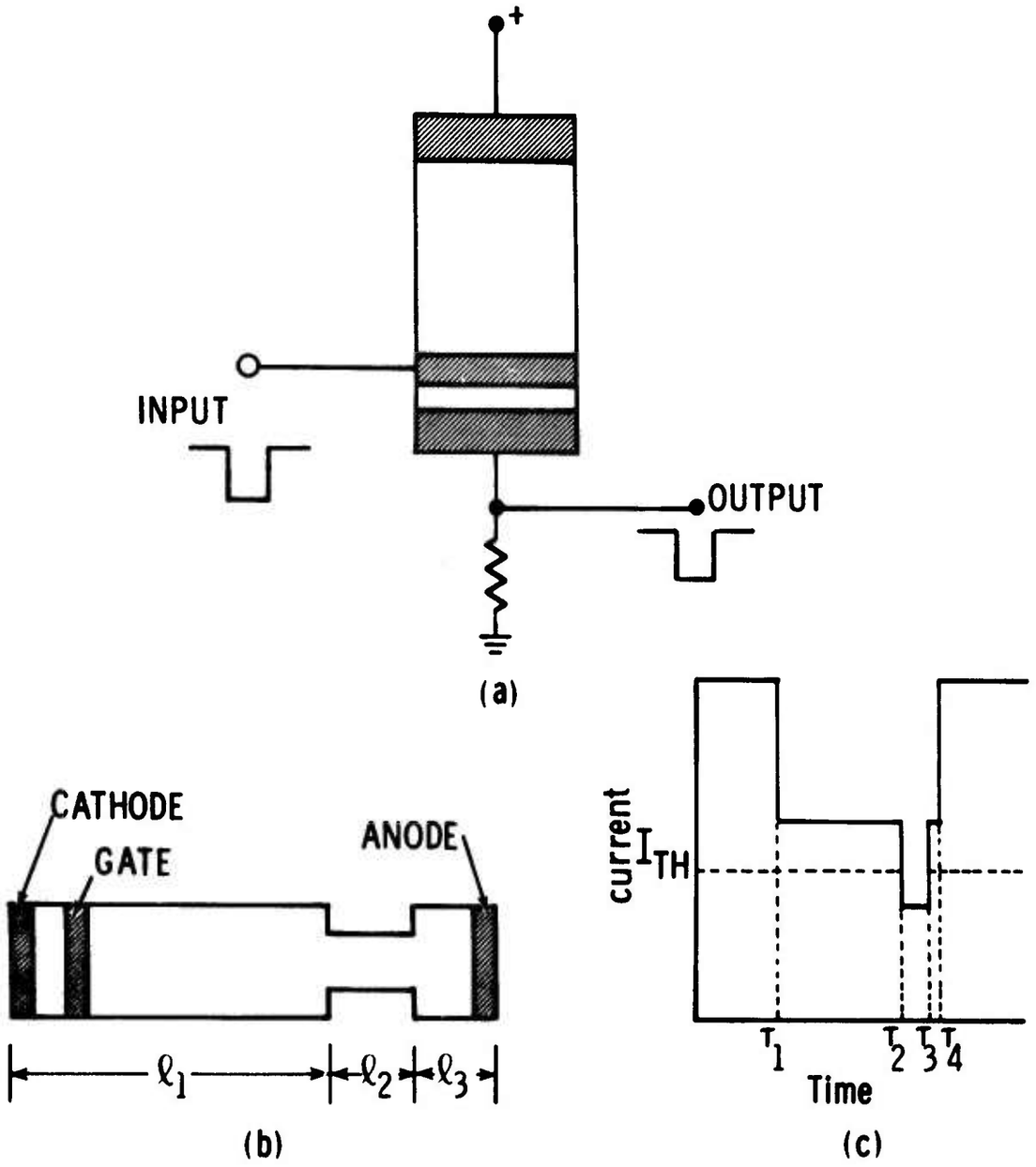

Figure 40. Basic Signal-Processing Circuit Using 3-Terminal TED. (a) three-terminal planar TED with notch near anode, (b) device geometry, and (c) device current as a function of time. The domain is nucleated at time τ_1, reaches the notch at time τ_2, leaves the notch at time τ_3, is absorbed at the anode at time τ_4.

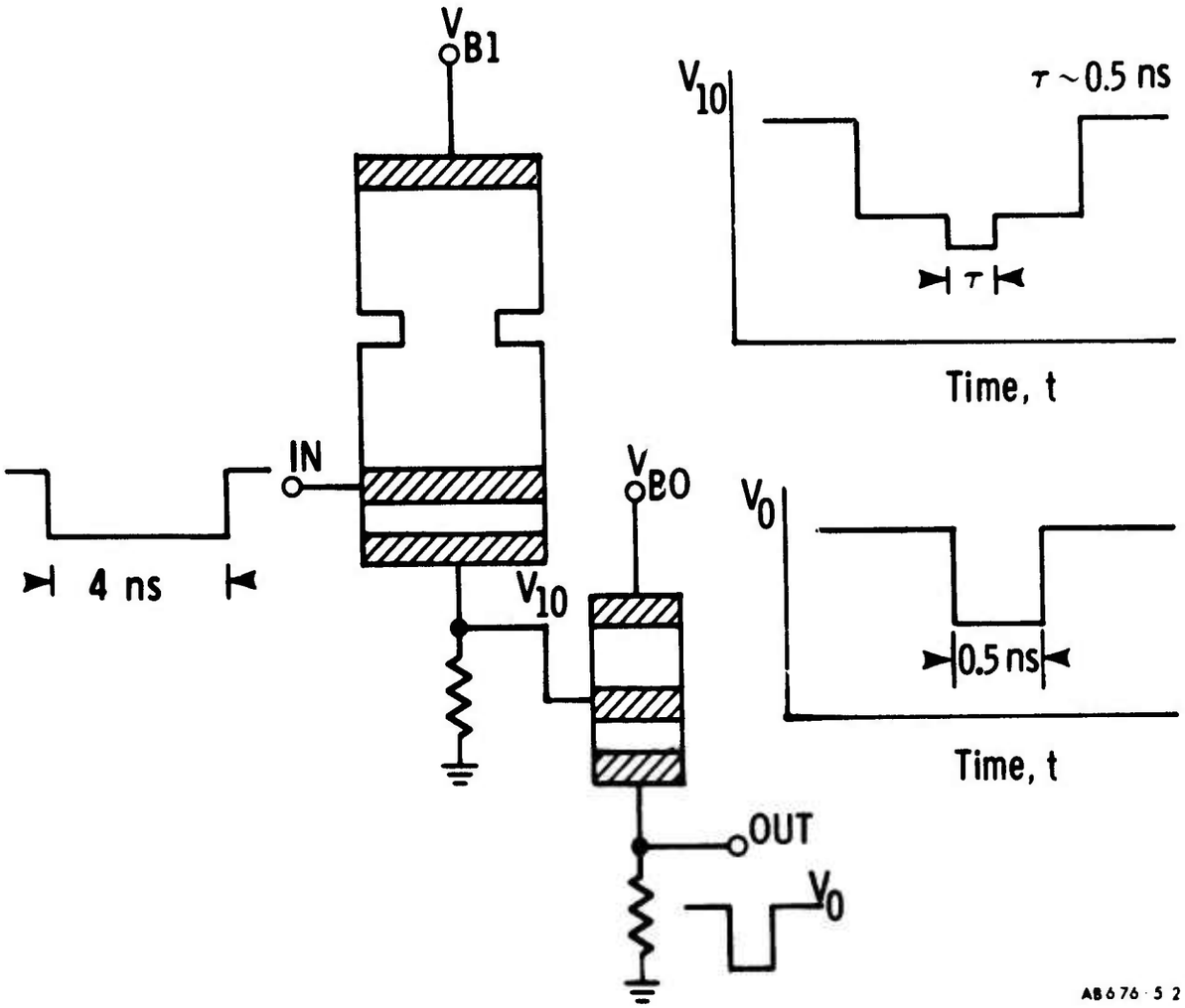

Figure 41. TED logic unit for 4-ns to 0.5-ns pulse-width conversion. TED input impedance is very high for negative input on the Schottky gate.

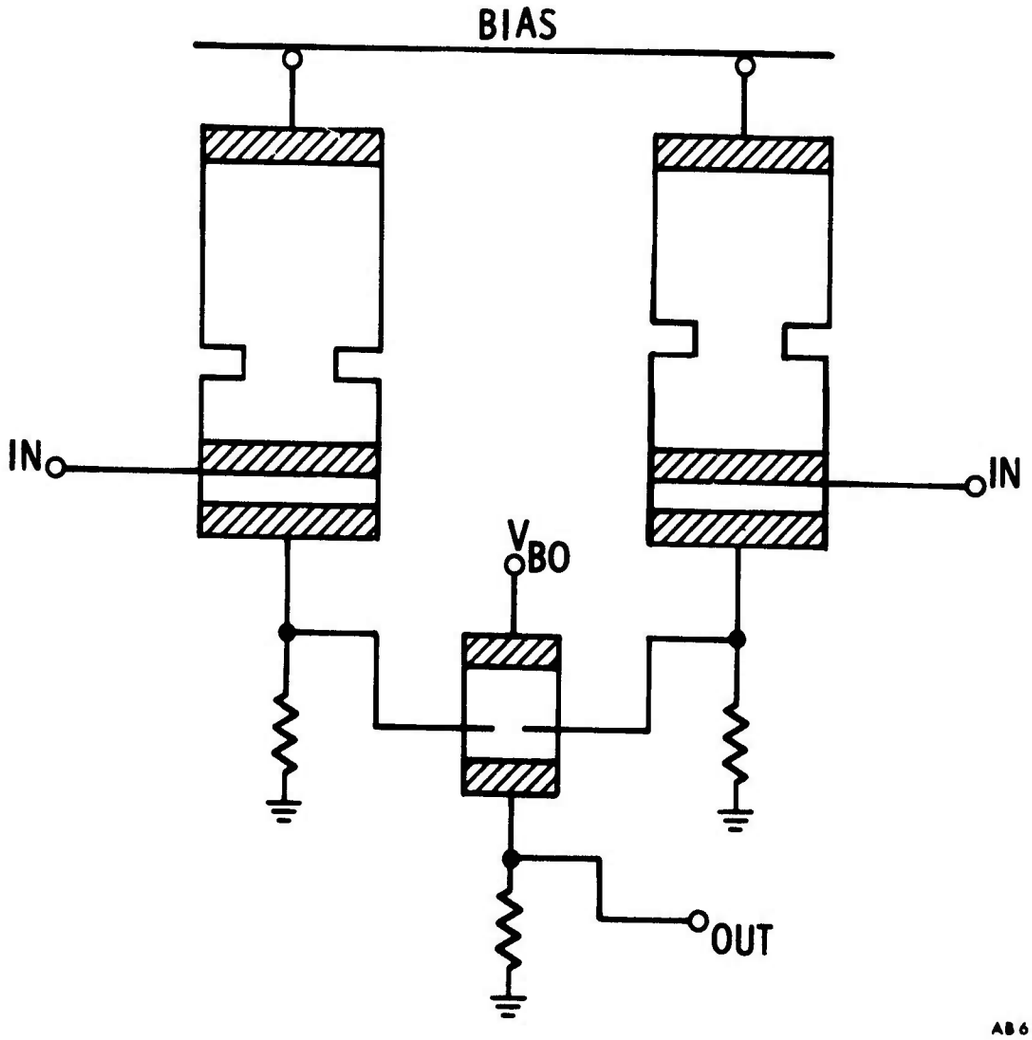

Figure 42. Schematic for a 2-bit multiplexer. An additional TED element may be needed between each input TED and the output TED.

manner, if eight input TEDs with 8 consecutive notches are used, complete multiplexing of 250 Mbit/sec input data on eight lines to a serial output with 2 Gbit/sec rate is achieved. Since this multiplexing may be rather complicated to fabricate, one can multiplex in two stages from eight lines to two lines and then from two to one line.

Although the above approach is fairly simple and should be realizable on a single GaAs chip, a further reduction in simplicity may be possible from the following consideration. The geometrical notches described above are used to selectively reduce the device area and hence increase the impedance in order to decrease the output current. These changes in resistance can also be achieved by using Schottky or MOS gates on one device. Figure 43 shows one input TED (with four Schottky gates) whose output drives an output TED in order to achieve a 4-bit multiplexer. For a 0.5-ns output pulse, the Schottky gates will be 0.25 ns wide and 0.25 ns apart, as shown. To estimate this width, we have $W = vt = 1.6 \times 10^7$ cm/sec x 0.25 ns = 40 μm. Such a gate width is clearly feasible. In addition, since the epi-GaAs layer is typically 2 - 5 μm, the Schottky gate can generate sharply-defined depletion regions so that the output pulse edge should be sharp. In this configuration each gate is used as an input port and the input TED is biased beyond the critical field. Extension to eight gates is straightforward.

The TED output is too low to satisfy the program requirements and an EBS amplifier will be required to increase the signal level to 5V. If the schematic of Figure 43 could be realized satisfactorily, a TED-multiplexer, EBS-amplifier combination may offer an attractive design for a high-data-rate multiplexer-PIN driver system due to the significantly reduced size, power consumption, and input drive power requirement.

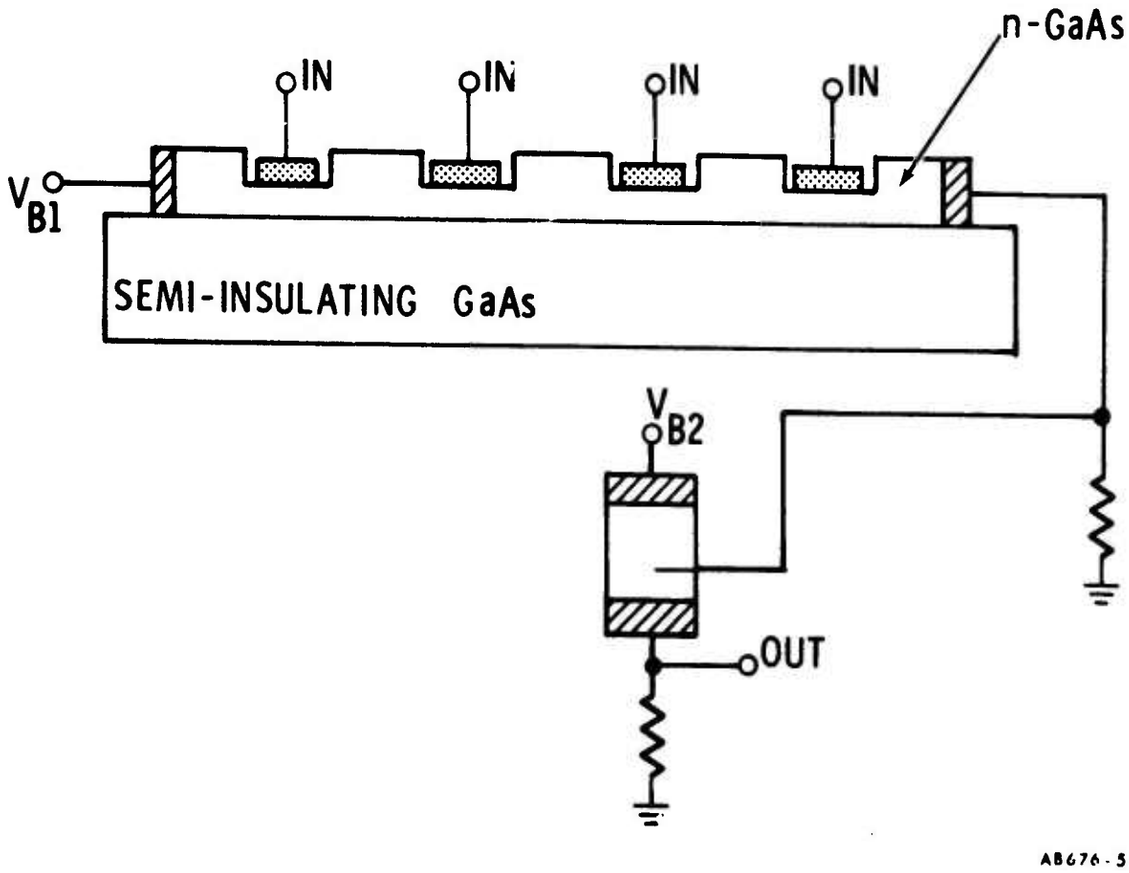

Figure 43. 4-Bit TED multiplexer with Schottky gate inputs. The steps in the GaAs epi may not be needed and are shown exaggerated for clarity.

SECTION VI
DEMULTIPLEXING CONSIDERATIONS

The Task III effort of the program involves the analysis and design of various approaches to demultiplexing a stream of 2 Gbits/sec serial data into eight lines (digital serial-to-parallel conversion), with a data rate of 250 Mbits/sec on each line. The input and output signal amplitudes are specified at 10 mV and 1V, respectively. We have considered two approaches to the problem: an EBS demultiplexer and a design which utilizes GaAs Transferred Electron Devices (TED) for the needed function.

6.1 EBS DEMULTIPLEXER DESIGN

The EBS demodulator demultiplexes a stream of 0.5 ns data pulses from a single line into 4 ns pulses on eight output lines. The device uses a CRT electron gun, a deflection system to produce a conically rotating electron beam, a conical (or cylindrical) pair of deflection plates or a helix for input data, and a target made of eight semiconductor diodes mounted in a circle concentric with the gun axis (see Figure 44). In steady-state, the beam traces a circle at the target plate just off the diodes. When an input pulse is present on the input deflection gate, the beam is deflected onto a target and produces an output signal (beam rotation must be synchronized with the input data). Hence, for eight diodes, 8 output pulses may be produced in one rotation period (4 ns) if the input includes eight 0.5 ns pulses in that time period.

For 0.5 ns input pulses, the electron beam strikes a target diode for only 0.5 ns. To achieve a 4-ns output pulse, one may utilize the frequency response characteristics of the EBS diode. The impulse response of a transit-time limited EBS diode is a square pulse of duration T, where T is the transit-time of the electrons across the diode depletion region. Therefore, the output pulse width can be controlled by the transit-time T. For a p+-n-n+ diode, T can be varied by the bias as long as the n-layer remains

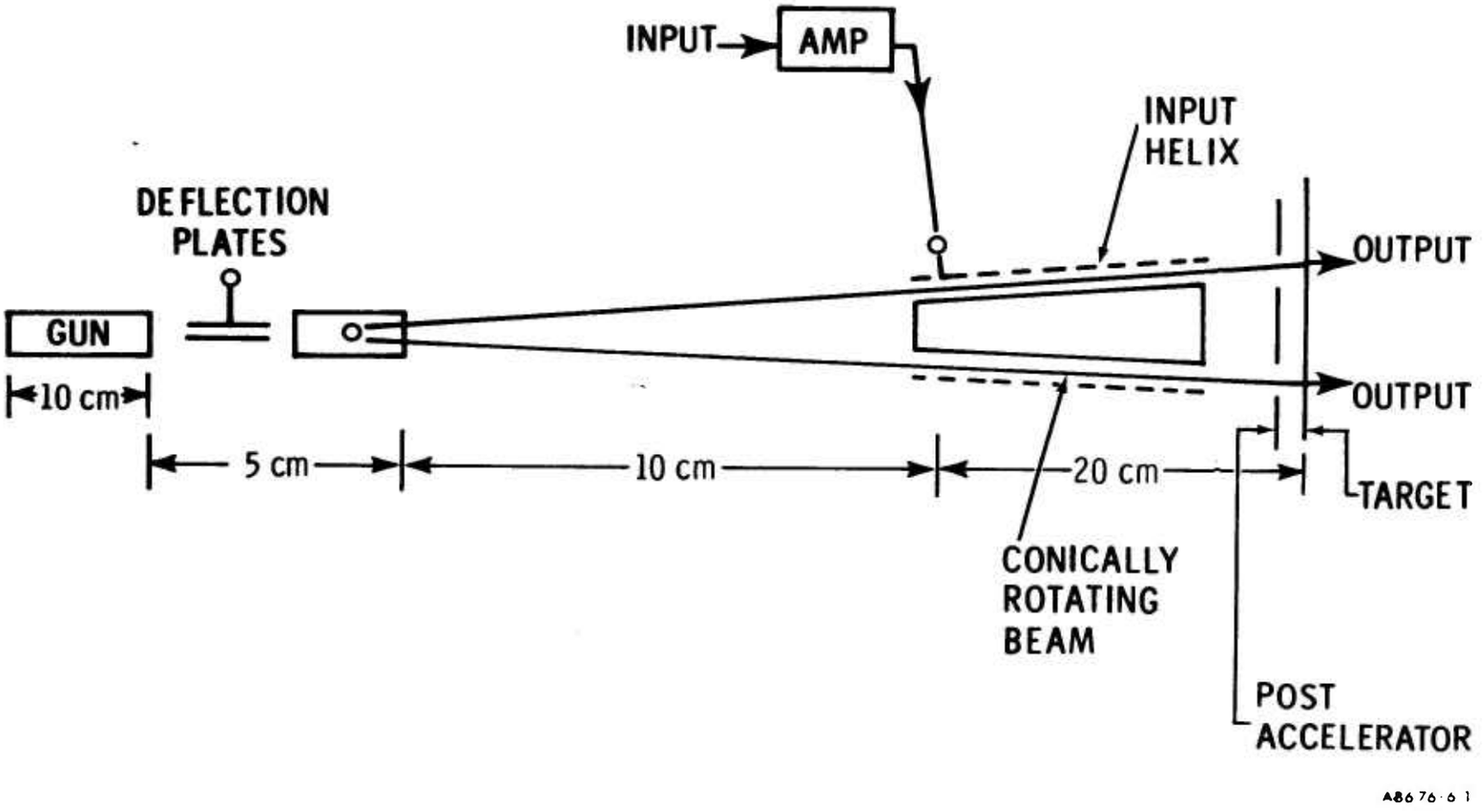

Figure 44. Schematic of the EBS demultiplexer design.

depleted. For $T < 4$ ns, one may use a transistor amplifier base storage-time delay to achieve 4 ns pulse-width. It must be noted that high frequency response is not an important consideration in the diode design. The electron beam reaches a specific target position for 0.5 ns every 4 ns. Therefore, for two consecutive pulses, the necessary requirement is that the charge created in the diode by the first electron pulse be collected before the second electron pulse strikes the diodes. This condition is satisfied for $T < 4$ ns. If the charge created in the diode is Q, the output current pulse amplitude is $\sim(Q/T)$. Therefore, T determines both the output pulse width and amplitude. Taking into account the RC limitations, it is then possible to arrive at an optimal target design.

The target may be deisnged for minimum rise-time with a transit-time of 2 ns. This is half the pulse-width of each output pulse and should provide a large signal amplitude at each output without overlap between two consecutive pulses. For minimum rise-time, we have

$$T = 2.97\,RC$$

Hence, for $R = 50\Omega$, the diode capacitance C is 13.5 pF. The junction width is

$$W = v_s T = 40\ \mu m$$

where we have assumed an electron velocity $v_s = 2 \times 10^6$ cm/s.

The diode area is

$$A = \frac{WC}{\epsilon} = 5.4 \times 10^{-2}\ cm^2$$

Assuming the electron beam is 1 mm in diameter, then each diode is a $1 \times 5.4\ mm^2$ strip. Allowing one beam width between two adjacent diodes, the target defines a circular array of 1.63 cm diameter.

The target peak output current is

$$I = \frac{Q}{T} = \frac{J_B A_B M \times 0.5}{2} \simeq 65 \text{ mA}$$

where a beam current density of $J_B = 50$ mA/cm^2, a target multiplication factor of M = 700, and a beam area of $A_B = 0.75 \times 10^{-2}$ cm^2 have been assumed.

The difficult part of the EBS demultiplexer is the deflection system for the input serial data. A traveling-wave helix with variable pitch will be needed since a single pair of deflection plates will not provide sufficient deflection amplitude. The helix is made in a cone section matching the angular rotation of the electron beam.

The electron transit-time through one segment of the helix should be less than the 0.5 ns input pulse width. For a transit-time of 0.25 ns and 4 kV electron beam (electron velocity of 3.8×10^9 cm/s), the width of the helix is

$$W_H = 3.8 \times 10^9 \times 0.25 \times 10^{-9} \simeq 1 \text{ cm}$$

The electron beam deflection amplitude at the target is then approximately given by

$$y = \frac{n W_H L V_{in}}{2g V_B}$$

where n is the total number of turns of the helix, L is the total electron travel distrance in field-free region, g is the helix gap above ground, V_{in} is the input voltage, and V_B is the beam voltage. For n = 6, L = 12 cm, g = 0.2 cm, V_B = 4 kV, and V_{in} = 2V, we obtain y = 0.9 mm, which is about one beam diameter. The total distance from the beginning of the helix to the target is $nW_H + L \simeq 18$ cm. Thus, a 2V input signal is needed for a 4 kV beam. A smaller input voltage is possible at a lower beam voltage. However, a lower current will be obtained at the target. The above calculations are for

feasibility considerations only, and the actual choice of the beam voltage should be decided more rigorously if such a device is to be built.

The deflection system for generating conical rotation of the beam and the electron gun are similar to the corresponding components in the digital multiplexer and therefore will not be discussed here.

Since the input data have 10 mV pulse amplitude, an amplifier will be needed to provide the 2V input signal. This amplifier will be required even if low beam voltages are used on the EBS demultiplexer. Assuming the transmission of the input data is synchronized to a clock, the clock signal may be used to generate the 250 MHz input signal for conical rotation, thus synchronizing the beam rotation to the input data.

Although an EBS demultiplexer appears conceptually feasible, the device size for this design is too large. A more attractive design, which should be especially more suitable for the low input voltages available, is presented below.

6.2 GaAs TED DEMULTIPLEXER DESIGN

GaAs TED devices have received considerable attention in recent years and show promise for high-data rate signal processing applications.[8-10] The TED device is a 3-terminal bulk GaAs sample with cathode, anode, and input gate electrodes. The device principle of operation is based on generating a high-field domain near the cathode which travels at electron saturation velocity across the device and is collected at the anode. The TED basic logic element was briefly described in Section V.

The TED demultiplexer design concept is shown in Figure 45. The input signal is amplified by a TED amplifier (more than one may be needed) to drive the eight TED AND gates in phase.[10] It will be assumed that a 250 MHz clock signal synchronized to the input data is available to supply enabling

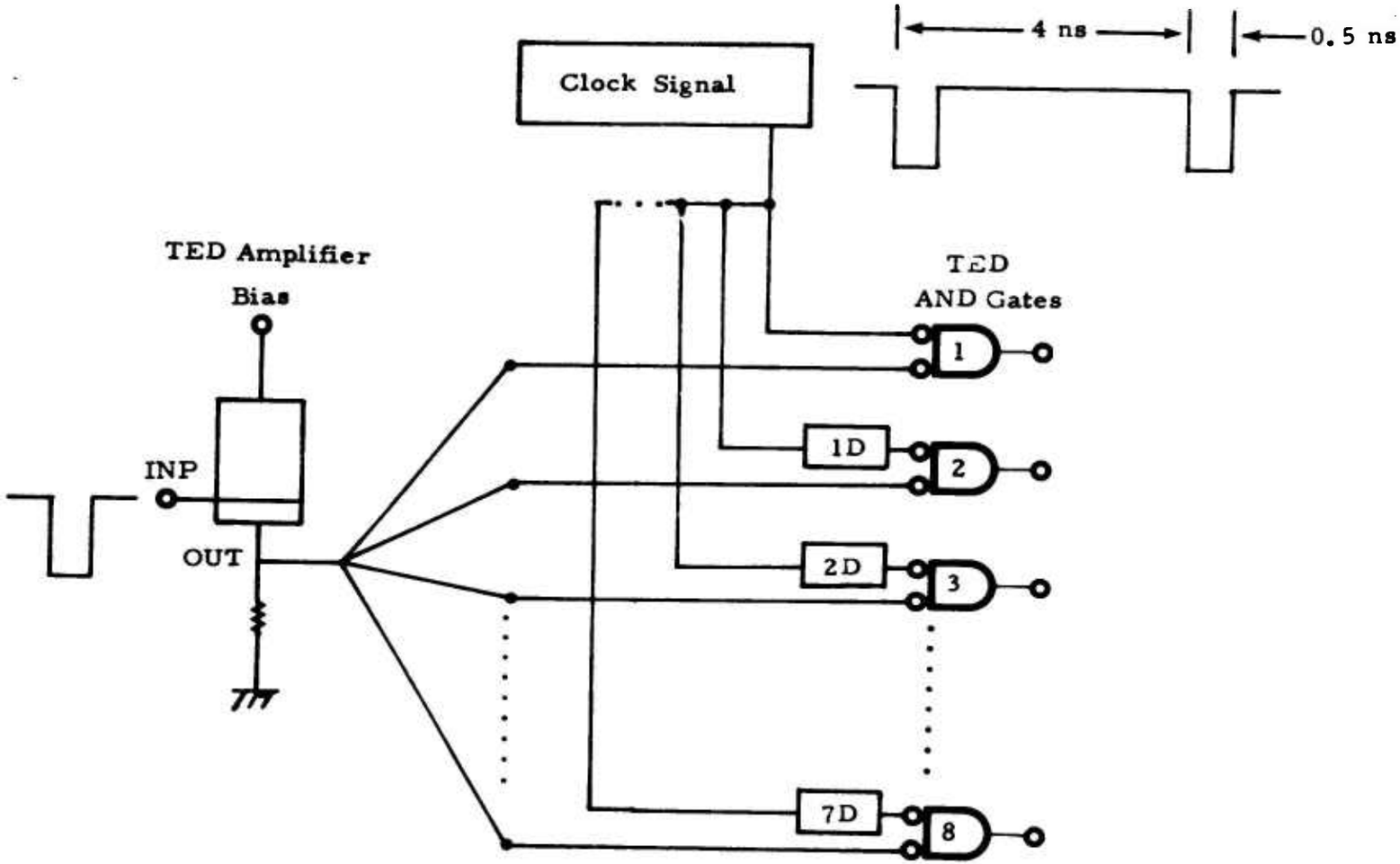

Figure 45. Schematic of a GaAs TED demultiplexer for 2 Gbits/sec input data.

signals to the eight AND gates. The clock pulse needed is 0.5 ns wide (one input data bit width) with 250 MHz repetition rate. The clock pulses can be generated by TED gates and possible methods of obtaining the clock signal will be considered later.

The AND gate output is in the 1 state when both its inputs are 1's. If one or both inputs are 0, the output is 0. Hence, if a clock signal arrives at an AND gate precisely synchronized with an input data pulse, the AND gate will provide an output pulse. Therefore, the clock signals to AND gates #2, 3, 4, . . . 8 need to be delayed relative to AND gate #1 by 0.5, 1, 1.5, . . . 3.5 ns, respectively, in order to obtain eight correct outputs on the eight AND gates in each 4 ns period. As an example, the input and output timing sequence for the eight gates for a 1-0 input data pattern is shown in Figure 46.

The output pulse width is decided by the AND gate design and may be 0.5 ns or longer. Final pulse amplitude and width to 4 ns can be achieved by a TED amplifier or a transistor switch, using the base storage time in saturation mode for pulse width widening. Both devices are capable of achieving the required function. If a TED amplifier is used, the total length of the TED will correspond to 4 ns travel-time at 10^7 cm/s electron saturation velocity, i.e., ~400 μm.

It should be noted that the outputs for the eight AND gates are consecutively 0.5 ns delayed since the input clock signals are delayed in the same format. If in-phase data are required on all the output lines, then the outputs of AND gates #7, 6, . . . 2, 1 should be delayed relative to gate #8 by 0.5, 1, . . . 3, 3.5 ns, respectively.

The delay required at the clock and AND gate outputs can be implemented by striplines or by additional TEDs.

The clock signals may be generated either from a 250-MHz sinusoidal signal synchronized to the serial data or from the data line itself. If the 250 MHz

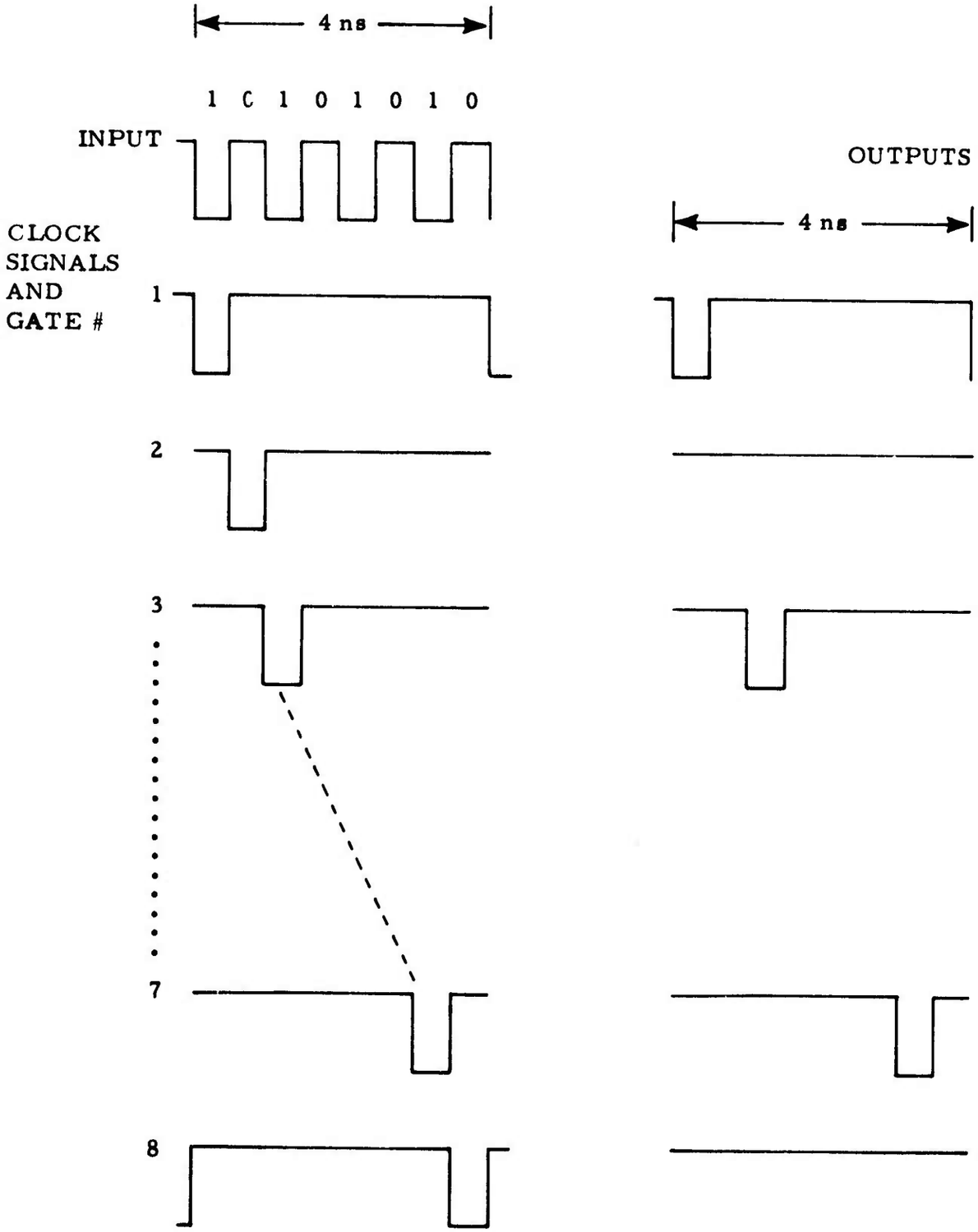

Figure 46. TED AND gates input, clock, and output patterns for a 1-0 input data pattern. The inputs to all ANDs are equal.

signal that drives the digital multiplexer is transmitted in-phase with the output serial data and received synchronously, driving a properly biased TED amplifier with this signal will generate the correct clock signal. The latter is then divided into eight lines and properly amplified and delayed by TED devices to drive the second inputs of the AND gates. Figure 47 shows the clock signal generation scheme. The TED length corresponds to 0.5 ns, i.e., 50 μm.

The input data pulse may itself by used to generate the enable signal. The schematic is shown in Figure 48. The input is amplified and divided into two lines, one going to the eight AND gates for demultiplexing. The other line drives a notched TED amplifier with 4 ns travel time. The output of the latter drives a 0.5-ns TED to generate the enable signal. The enable signal is then amplified, etc., as described in the previous paragraph. In this scheme, the input signal must be delayed by a specific amount due to the delay involved in generating the clock pulse. This will synchronize the input data and the enable pulses so that, for instance, bit #1 and enable pulse #1 arrive at AND-gate #1 at precisely the same time. It should be noted that this scheme can be used only in a regenerative mode. That is, the first data bit received is used to trigger the clock on. A TED memory cell is needed before the 4-ns TED of Figure 48. and in this sense, the first data bit is used as a SET signal. For a description of TED memory cell the reader is referred to Section II-C of Ref. (10).

The demultiplexing scheme described above is totally realized in TEDs and could be implemented on a single GaAs chip. The basic functions of TED logic devices and amplifiers have been demonstrated experimentally,[8-10] and therefore the above scheme, with proper TED design at each stage, should be feasible.

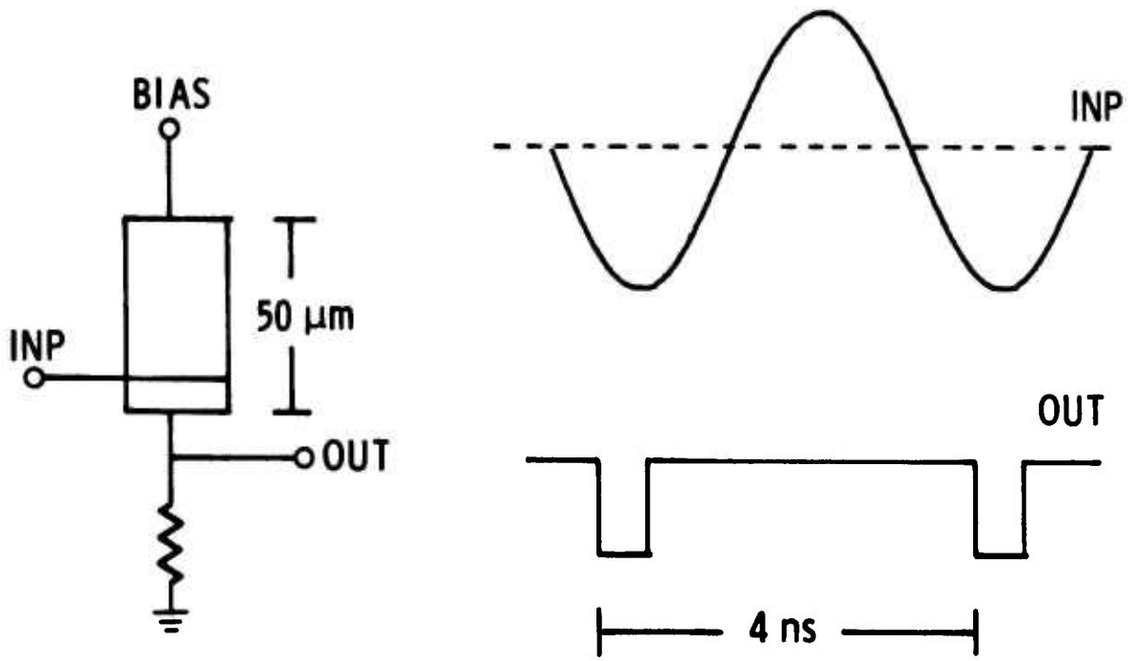

Figure 47. Generation of the clock signal from a 250 MHz sinusoidal signal.

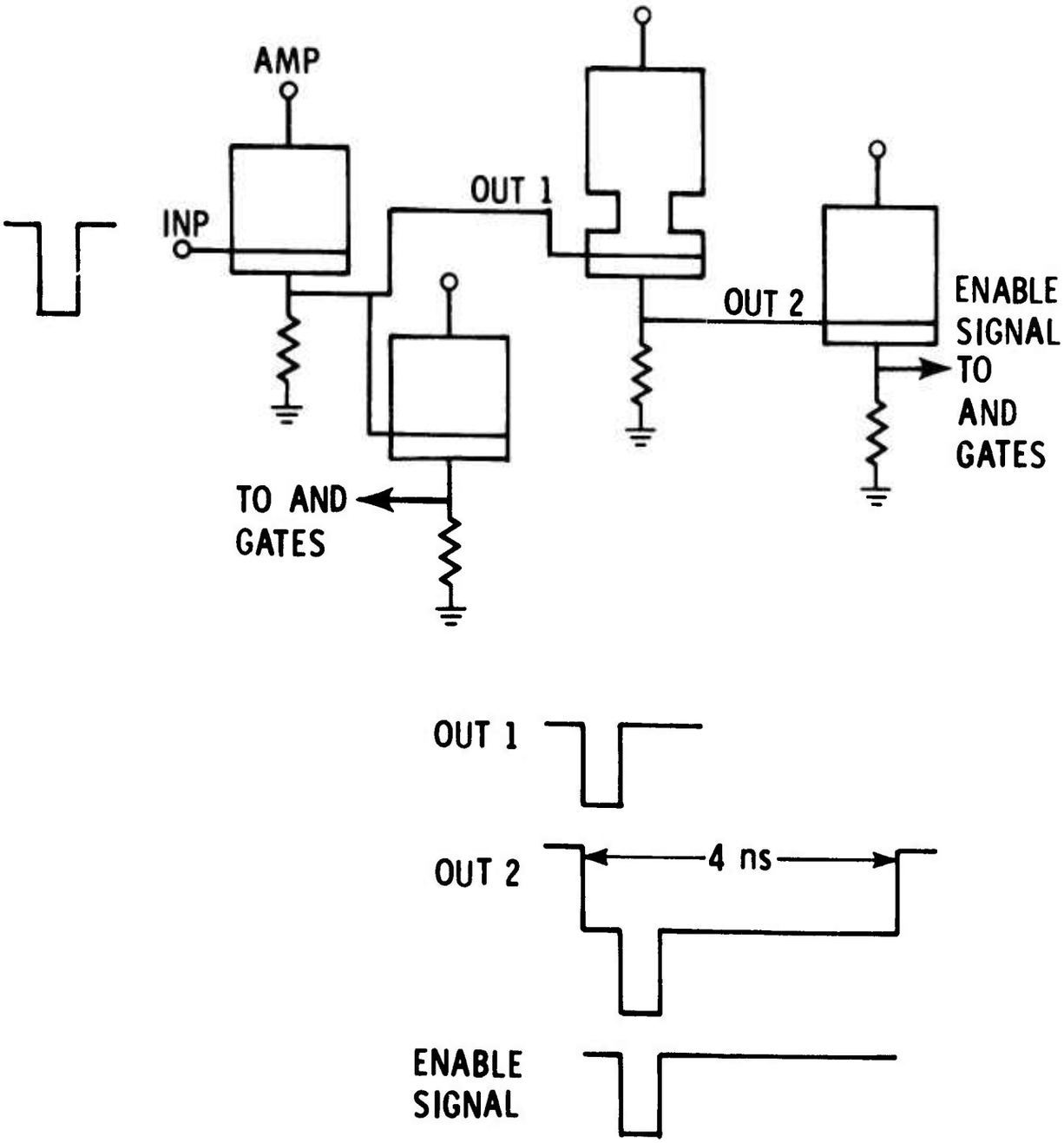

Figure 48. Generation of the clock signal to Enable AND gates from the input data.

SECTION VII

CONCLUSIONS AND FUTURE EFFORT

The program objectives in the development of a 2 Gbits/sec EBS digital multiplexer have been essentially met. The signal amplitude achieved exceeds the program specifications. The output pulse rise-time for the single-gun, single-target design was generally about 0.25 ns and lower than the specified value of 0.2 ns, though the output pulses corresponding to some gates did show 0.2 ns 10 - 90% rise-time. In addition, the results of this program show very significant improvements over previous work, where an EBS multiplexer was fabricated for the first time with very limited funds and time.[6] The output data for the multiple-gun design indicate fast rise-time and up to 7V pulse amplitude. The rise-time was typically 0.2 ns.

On the basis of the results achieved for the two designs, the multiple-gun, single-target approach appears to offer better performance and should also have lower manufacturing cost. Very precise alignment and a good conical beam rotation pattern are essential to the proper operation of the single-gun multiplexer. On the other hand, beam rotation is not used in the multiple-gun design, and precise alignment is not a necessary condition to its operation.

The single-gun multiplexer could be reduced in size if the beam radius and the size of the gate structure were reduced. However, a smaller gate structure would intensify alignment and beam rotation problems. A very small gap between the gate and ground would require a small beam diameter, an exceedingly precise circular rotation pattern, and very good alignment. These conditions are difficult to achieve.

For future work, a four-gun device could be fabricated in still smaller tube envelope. A reduction in length from 25 cm to 20 cm seems quite feasible. In addition, if cold cathodes with sufficient current emission can be developed, a very compact multiple-gun, single-target multiplexer may become feasible.

REFERENCES

1. H. Kuno, Y. Chang, and D. English, Air Force Avionics Laboratory Report AFAL-TR-74-175, May 1974.

2. C. Norris, Jr., "Optimum Design of EBS Low-Pass Amplifiers -- Part I: Bandwidth and Rise Time," IEEE Trans. Elect. Devices, ED-20, 447 (1973).

3. A. S. Grove, Physics and Technology of Semiconductor Devices, John Wiley and Sons, Inc., N. Y. (1967).

4. T. Everhart and P. Hoff, "Determination of Kilovolt Electron Energy Dissipation vs Penetration Distance in Solid Materials," J. Appl. Phys. 42, 5837 (1971).

5. W. E. Armstrong and D. L. Tolliver, "A SEM Investigation of Glass Flow in MOS IC Fabrication," J. Electro-Chem. Soc. 121, 307 (1974).

6. A. Bahraman and G. Dohler, Air Force Avionics Laboratory Technical Report AFAL-TR-73-167, June 1973.

7. A. El-Kareh and M. Sturans, "Analysis of 3-Tube Symmetrical Electrostatic Unipotential Lens," J. Appl. Phys. 42, 1870 (1971).

8. F. Sterzer, "Information Processing with Transferred-Electron Devices," RCA Review 34, 152 (1973).

9. M. Takeuchi, A. Higashisaka, and K. Sekido, "GaAs Planar Gun Diodes for DC-Biased Operation," IEEE Proc. 60, 740 (1972).

10. S. Narayan, L. Upadhyayula, M. Nowogrodzki, and R. Smith, Air Force Avionics Laboratory Technical Report AFAL-TR-73-321, Sept. 1973. Also see: L. C. Upadhyayula and R. E. Smith, Technial Report AFAL-TR-75-140.

☆ U. S. GOVERNMENT PRINTING OFFICE: 1977 — 757-001/342